Pamukkale Univ Muh Bilim Derg, XX(X), XX-XX, 20XX

Pamukkale Üniversitesi Mühendislik Bilimleri Dergisi

Pamukkale University Journal of Engineering Sciences

INFO algorithm based MPPT optimization of a photovoltaic system under partial shading conditions

Kısmı gölgelenme koşulları altında fotovoltaik sistemlerin INFO algoritması tabanlı MPPT optimizasyonu

Kezban Koç Savaş[1], Mehmet Demirtaş[1], İpek Çetinbaş[2]*

[1]Department of Electrical and Electronics Engineering, Faculty of Technology, Gazi University, Ankara, Türkiye.
kezbankoc@gazi.edu.tr, mehmetd@gazi.edu.tr

[2]Department of Electrical and Electronics Engineering, Faculty of Engineering and Architecture, Eskisehir Osmangazi University, Eskisehir, Türkiye.
ipekcetinbas@ogu.edu.tr

Received/Geliş Tarihi: 22.01.2025 Revision/Düzeltme Tarihi: 26.08.2025 doi: 10.65206/pajes.79484
Accepted/Kabul Tarihi: 08.10.2025 Research Article/Araştırma Makalesi

Abstract

Obtaining maximum efficiency from photovoltaic (PV) systems through maximum power point tracking (MPPT) remains an ongoing challenge. In this study, the weighted mean of vector (INFO) algorithm is employed to address and solve the MPPT problem for a photovoltaic system operating under partial shading. Besides INFO algorithm, electric eel optimization (EEFO), red-tailed hawk algorithm (RTHA), and student psychology-based optimization (SPBO) algorithms were also employed, and this study is the first to employ these optimization algorithms for MPPT purposes. The particle swarm optimization (PSO) algorithm, which is frequently employed in MPPT studies, is employed to compare the performance of new metaheuristic algorithms. These algorithms are tested with challenging shading scenarios where the local maximum points (LMPPs) and global maximum power point (GMPP) varied. The performance of these algorithms is evaluated using the Friedman test, which is a statistical test, and performance metrics. According to the findings of the comparison, the INFO algorithm is the most effective among the five algorithms for MPPT optimization under partial shading conditions, and this conclusion is confirmed statistically. Additionally, experimental tests were conducted to evaluate the performance of the INFO algorithm on real hardware. A programmable PV simulator, boost converter, and STM32 board were used. The experiments demonstrated that the algorithm could quickly and stably track the maximum power point.

Keywords: Friedman Test, INFO, Maximum Power Point, MPPT, Partial Shading, Photovoltaic.

Öz

Fotovoltaik (FV) sistemlerden maksimum verim elde etmek için maksimum güç noktası izleme (MPPT) yöntemi önemli bir araştırma konusu olmaya devam etmektedir. Bu çalışmada, kısmi gölgeleme koşulları altında çalışan bir FV sistem için MPPT problemini çözmek amacıyla vektörlerin ağırlıklı ortalaması (INFO) algoritması kullanılmıştır. INFO'ya ek, elektrikli yılanbalığı optimizasyonu, kızıl kuyruklu şahin algoritması ve öğrenci psikolojisine dayalı optimizasyon algoritması da uygulanmış olup, söz konusu optimizasyon algoritmaları MPPT amacıyla ilk kez bu çalışmada kullanılmıştır. Yeni meta sezgisel algoritmaların performansını karşılaştırmak amacıyla, MPPT çalışmalarında yaygın olarak kullanılan parçacık sürü optimizasyonu algoritması da kullanılmıştır. Algoritmalar, yerel maksimum güç noktalarının ve küresel maksimum güç noktasının değişkenlik gösterdiği zorlu gölgeleme senaryolarında test edilmiştir. Algoritmaların performansları, istatistiksel bir test olan Friedman testi ve performans metrikleri kullanılarak değerlendirilmiştir. Karşılaştırma sonuçlarına göre, kısmi gölgeleme koşulları altında MPPT optimizasyonu için en etkili algoritmanın INFO algoritması olduğu belirlenmiş ve bu sonuç istatistiksel olarak doğrulanmıştır. Ayrıca, INFO algoritmasının gerçek donanımda performansını test etmek için deneysel çalışmalar yapılmıştır. Programlanabilir FV simülatörü, yükseltici tip dönüştürücü ve STM32 kartı kullanılmıştır. Deneyler, algoritmanın hızlı ve kararlı şekilde maksimum güç noktasını izlediğini göstermiştir.

Anahtar kelimeler: Friedman Testi, INFO, Maksimum Güç Noktası, MPPT, Kısmi Gölgeleme, Fotovoltaik.

1 Introduction

1.1 Theoretical background and research gap

The advancements in technology and the increasing human population are causing a rise in the demand for electrical energy. If the consumption of electrical energy keeps rising at this rate, it is expected that by the year 2050, the world's installed power will need to be twice as much as the current installed power [1]. Since it is not possible to meet the increasing energy demand entirely from fossil fuels, there has been a search for alternative sources to these resources. Due to the impossibility of meeting the energy demand solely through fossil fuels, there has been a search for alternative resources. In this direction, scientists and investors have turned to cleaner, more environment-friendly energy resources that do not emit carbon during production [2],[3]. Some of the most significant renewable energy sources are wind, solar, biomass, hydroelectric and wave. Among these, solar and wind the most utilized sources for electricity production due to their accessibility [4]. There was a 14% increase in the use of wind and a 26% on the rise in the use of solar in 2022 compared to the last year, as revealed by the statistics of the International Energy Agency [5].

PV systems are the most common application for harnessing solar energy to produce electrical energy [6]. PV systems offer numerous advantages, including directly converting solar energy into electrical energy, long-term usage guarantee, lower maintenance and repair costs, and the absence of moving components [2], [3]. With the decline in the production and

*Corresponding author/Yazışılan Yazar

initial installation costs of PV systems, their areas of use are growing [6]. Although the sun has an enormous energy potential, this potential cannot be fully harnessed and converted into electrical energy. Despite being claimed to be 25% under laboratory circumstances, the practical efficiency of an average PV array remains below 20% in practice. Therefore, most researchers working on PV systems aim to increase this efficiency rate. Multiple factors affect the efficiency of PV arrays, such as temperature, radiation, shading, and the type and quality of the materials used [7]. The most frequently utilized method to increase the efficiency of PV arrays is to identify the point at which the array operates at maximum power (this point is called the maximum power point) and then use an algorithm to operate the array continuously at this point.

The objective of utilizing MPPT approaches is to reduce the oscillations induced by variations in temperature and irradiation on the power-voltage (P-V) graph. This approach allows PV systems to consistently achieve optimal power generation, resulting in the highest achievable benefit [8]. When there is no shade in PV systems, a single MPP is formed on the P-V graph. However, when shading occurs, multiple MPPs are formed. In such graphs, one GMPP and multiple LMPPs can be observed. The MPPT method employed under partial shading conditions must be able to operate at the GMPP without getting stuck at the LMPPs.

1.2 Literature review

Upon reviewing the literature on MPPT, it is evident that various methods are presented. These can be categorized as seven categories: traditional methods, fixed parameter methods, artificial intelligence-based methods, mathematical-based methods, methods utilizing characteristic graphs, hybrid methods, and metaheuristic algorithm-based methods [9], [10]. The categorized MPPT methods are presented in Figure 1. The first MPPT category is traditional methods, which are divided into three subcategories. These are called perturb & observe [11], [12], hill climbing [13], [14], and incremental conductance methods [15]. Although traditional methods are easy to use, they tend to get stuck at LMPPs under partial shading conditions, resulting in a decrease in efficiency [16]. The second category consists of methods based on a fixed parameter, with the most popular being open circuit voltage [17], short circuit current [18], constant current and voltage methods [19]. These methods utilize the behavior of PV panel parameters according to changes in irradiation and temperature. In particular, the short circuit current method is greatly affected by temperature. Since it requires periodic measurement of voltage or current, it necessitates frequent switching. This situation increases the cost while reducing efficiency [20]. The third group comprises techniques that are based on artificial intelligence. The most frequently employed techniques include fuzzy logic controllers [21], artificial neural networks [22], and machine learning algorithms [23]. Mathematical-based approaches in the fourth category include Chaotic search [24] and beta algorithm [25]. These algorithms exhibit significant computational complexity and slow convergence rates [9]. The fifth category comprises methods that use characteristic curves, which divide the P-V graph into trapezoidal regions. These methods have long response times and low efficiency in shading scenarios with three or more peak points [26-28]. The final category encompasses hybrid approaches. Hybrid approaches, which involve the combined use of two distinct traditional techniques or the combination of conventional methods with metaheuristic methods. Hybrid studies, which appear frequently in the literature, seek to capitalize on the advantages of various approaches [29-32].

Upon reviewing the current literature, it is evident that there has been a substantial increase in studies using MPPT utilizing metaheuristic algorithms, particularly in recent years. Due to their ease of understanding and implementation, metaheuristic algorithms can be easily applied to engineering problems. The solutions they provide for intricate optimization problems are particularly satisfactory [33]. In the literature, 19 valuable studies solving the MPPT optimization problem using metaheuristic algorithms have been reviewed.

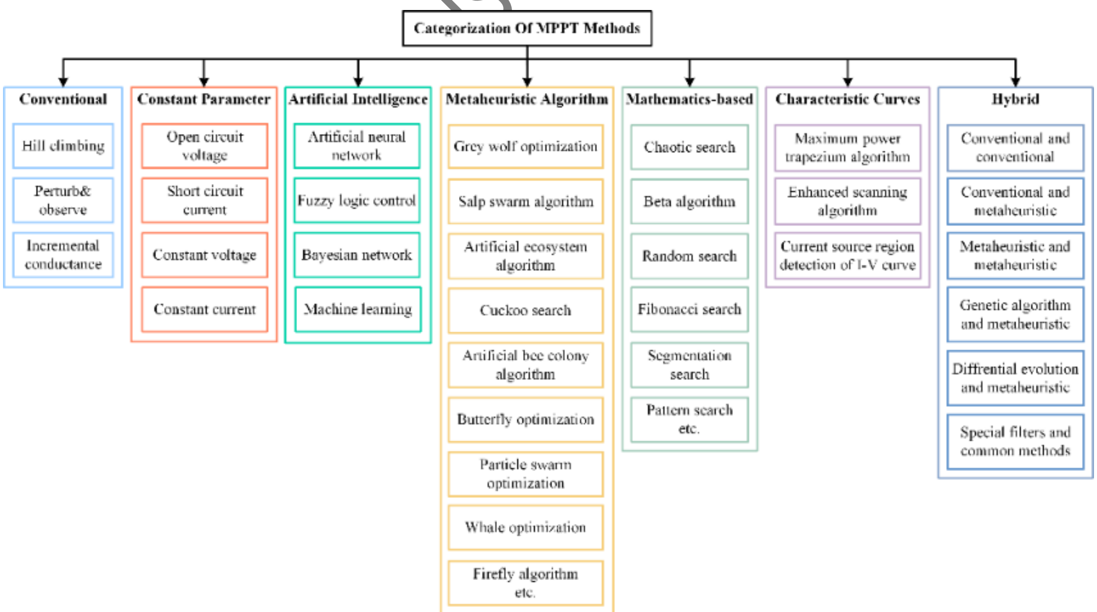

Figure 1. Categorization of MPPT methods.

These algorithms include the combination of artificial bee colony and teaching learning algorithm [2], sine-cosine algorithm [34], honey badger algorithm [35], squirrel search algorithm [36], harris hawk optimization [37], falcon optimization algorithm [38], hierarchical pigeon-inspired optimization [39], dynamic group based cooperation optimization [40], grasshopper optimization algorithm [41], most valuable player algorithm [42], improved mayfly algorithm [43], modified particle swarm optimization algorithm [44], modified rat swarm optimization [45], yellow saddle goatfish algorithm [46], tuna swarm optimization algorithm [47], horse herd optimization [48], henry gas solubility optimization [49], ant lion optimization [50], and salp swarm optimization [51]. The detailed presentation of this literature review is provided in Table 1. This table provides comprehensive data on the algorithm, comparison algorithm/s, converter type, configuration type (where S denotes series connected arrays and P denotes parallel-connected arrays), number of scenario/s, GMPP location (including details on dynamic fast change irradiance (DFCI)), simulation/experimental setup, and statistical test/s.

Table 1. Literature review

Algorithm	**Comparing Algorithm/s**	**Converter Type**	**Configuration Type**	**Number of Scenarios**	**GMPP Location**	**Simulation/ Experimental**	**Statistical Test/s**
Combination of teaching learning and artificial bee colony [2]	Improved grey wolf optimization (IGWO) PSO Moth flame optimization Salp swarm optimization algorithm (SSOA) Perturb and observation (P&Q) Variable step size incremental conductance Adaptive P&Q and fuzzy logic control	Boost	4S3P	4	Standard test condition (STC) Right Middle on right Middle on left	Simulation/ Experimental	-
Sine-cosine algorithm [34]	SSOA P&Q	CUK	4S1P	4	Middle on left DFCI (4s)	Simulation	-
Honey badger optimization [35]	PSO P&O	Boost	4S1P 4S2P 4S3P 3S3P 2S4P	5	N/A	Experimental	-
Improved squirrel search algorithm [36]	Squirrel search algorithm (SSA) Genetic algorithm PSO Ant colony optimization-P&Q Overall distribution PSO Artificial bee colony (ABC)	Boost	3S1P	5	Right Middle Left DFCI	Simulation/ Experimental	-
Harris hawk optimization [37]	PSO Dragonfly optimization algorithm (DFOA) GWO P&O	Boost	4S1P 12S1P	4	DFCI (2s) GMPP and LMPPs too close	Simulation	-
Falcon optimization algorithm [38]	PSO P&O	Boost	4S1P	4	STC Left Middle on right Right	Simulation	Friedman Test Wilcoxon Test
Hierarchical pigeon inspired optimization [39]	Modified firefly algorithm Deterministic PSO (DPSO) Overall distribution Cubic spline guided Jaya Modified incremental conductance Pigeon inspired optimization	Boost	5S1P	4	STC Right Left (2nd peak) Middle on right	Simulation/ Experimental	-
Dynamic group based cooperation optimization [40]	DragonFly optimizer ABC Cuckoo search algorithm (CSA) PSO	Boost	4S1P	4	DFCI (2s) Middle Left Right	Simulation	-
Grasshopper optimization algorithm [41]	P&O Differential evolution PSO	Boost	2S3P	3	N/A	Experimental	-

Table 2. (continued)

Algorithm	Comparing Algorithm/s	Converter Type	Configuration Type	Number of Scenarios	GMPP Location	Simulation/ Experimental	Statistical Test/s
Most valuable player algorithm [42]	Modified Jaya algorithm PSO	Boost	4S1P	4	N/A	Simulation/ Experimental	-
Improved mayfly algorithm [43]	PSO	Boost	4S1P	2	Standard test condition (STC) Middle on right	Simulation/ Experimental	-
Modified particle swarm optimization [44]	Bat algorithm (BAT) IGWO PSO P&Q	Buck	2S1P 4S1P	6	Left Right Right Middle Middle on right DFCI (1s)	Simulation/ Experimental	-
Modified rat swarm optimization [45]	Fireworks algorithm and P&Q Flower pollination algorithm P&Q	Boost	4S1P	6	DFCI (1s) Right Middle Middle on right Right Left (2nd peak)	Experimental	-
Yellow saddle goatfish algorithm [46]	BAT GWO PSO Seagull optimization algorithm	Buck-Boost	4S1P 6S1P	5	DFCI (5s)	Simulation	-
Tuna swarm optimization algorithm [47]	PSO Squirrel Search Algorithm Black widow spider optimization algorithm	Boost	5S1P	6	Left Middle Right Middle on right Middle Left	Simulation	-
Horse herd optimization [48]	GWO PSO Flower pollination algorithm DPSO CSA	Boost	4S2P	6	DFCI (2s) Right Middle on right Middle on left Left	Simulation/ Experimental	-
Henry gas solubility optimization [49]	DFOA PSO Grasshopper optimization P&Q CSA	Boost	4S1P 12S1P	4	DFCI (2s) Right Middle on left GMPP and LMPPs too close	Simulation	-
Ant lion optimizer [50]	P&Q Flower pollination algorithm	N/A	N/A	2	STC Dynamic- fast changing irradiance and temperature	Simulation	-
Salp swarm optimization [51]	DFOA ABC PSO-Gravitational Search CSA P&Q PSO	Boost	4S1P 12S1P	5	DFCI (2s) Middle on right Middle on left GMPP and LMPPs too close	Simulation/ Experimental	-

1.3 Motivation and major contributions

Upon thorough evaluation of the literature presented in Table 1, it is evident that various algorithms, methods, and approaches exist to address the MPPT problem. However, it is essential to take into account that no single approach is capable of handling all the associated challenges [52-53]. In accordance with the no-free lunch theory, no single metaheuristic algorithm can solve all problems with equal success [54]. In this study, the INFO, EEFO, RTHA, SPBO, and PSO algorithms were selected to address the MPPT problem. In addition, the focus was not only on how accurately the optimization algorithms produced the best result once but also on how consistently they demonstrated the same successful performance. For this purpose, all algorithms were subjected to statistical testing. The main contributions of this study to the literature are given below.

- This study employed the INFO, EEFO, RTHA, and SPBO algorithms for the first time in the literature to address the MPPT problem.
- To better examine the performance of selected algorithms, the GMPP point's position in the P-V graph was adjusted to be on the right, middle, and left positions in the tested scenarios. Additionally, LMPPs and GMPP were positioned very close to each other to increase the difficulty of the tested scenarios.
- The INFO, EEFO, RTHA, SPBO, and PSO algorithms were compared using evaluation metrics and statistical test called Friedman test.
- The INFO algorithm performed better than the others based on both evaluation metrics and the Friedman test. This reinforces the success and consistency of the INFO

algorithm in resolving the MPPT optimization problem.

- The INFO algorithm was experimentally validated under partial shading condition, confirming its real-world applicability.

1.4 Organization of the article

This study consists of six sections. Following the Introduction, Section 2 presents the definition of the MPPT optimization problem. Section 3 explains the INFO algorithm in detail, followed by brief summaries of the EEFO, RTHA, SPBO, and PSO algorithms. The simulation results are given in Section 4. Section 5 provides the experimental validation of the INFO algorithm under partial shading conditions. Finally, Section 6 presents the conclusions of this work and discusses potential future studies.

2 Definition of the MPPT optimization problem under partial shading conditions

The main goal of this paper is to implement MPPT for a PV system that operates partial shading conditions. For this purpose, a PV system consisting of a PV array, DC-DC boost converter, MPPT controller, and load components has been designed and presented in Figure 2. The evaluation criteria for these components and algorithms are provided in the subsections.

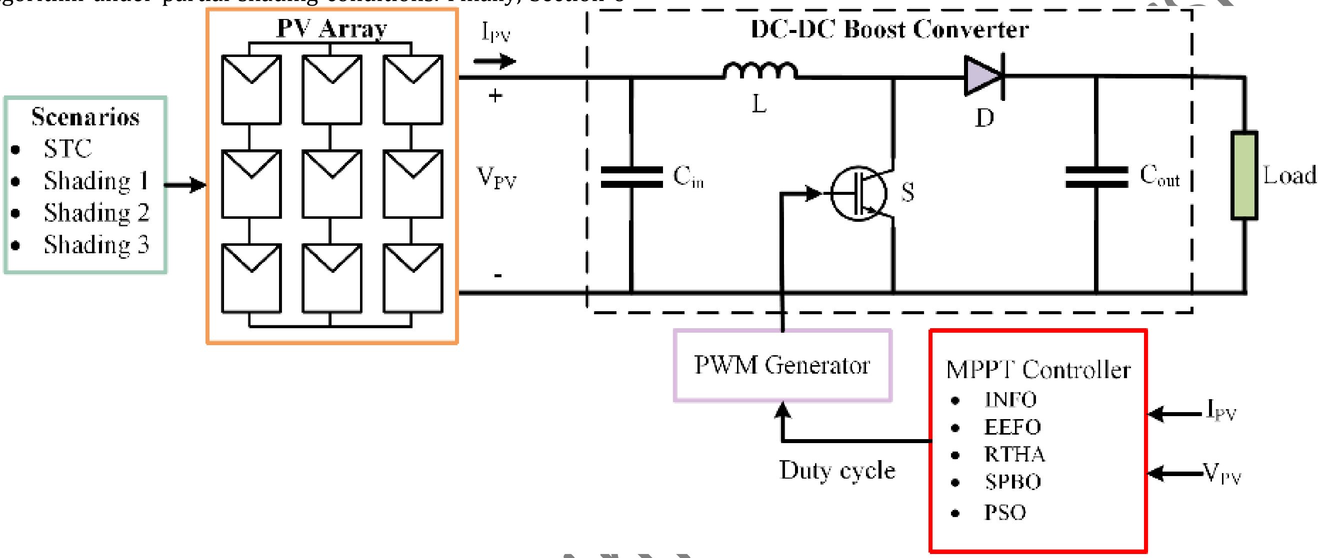

Figure 2. PV system and component .

2.1 PV cell and module

A PV cell is the smallest element in the PV arrays. These cells are connected to each other either in series or in parallel to form the PV modules. In the literature, there are different models for the electrical equivalent circuit of a PV cell. In this study, the single-diode model is selected due to its simplicity, accuracy, and frequent usage. In Figure 3, the electrical equivalent models of a single diode PV cell, PV module, and PV array are presented. The single-diode equivalent model consists of a current source (I_{ph}), a diode, parallel (R_{sh}), and a series resistance (R_s). The mathematical expressions for the cell's output current and diode current are given in Equations (1)-(2). Equation (3) provides the mathematical expression for the junction thermal voltage (V_t).

$$I_{cell} = I_{ph} - I_d - I_{sh} \tag{1}$$

$$I_d = I_0 \times \left[e^{\left(\frac{V+I_{cell}\times R_S}{\alpha\times V_t}\right)} - 1\right] \tag{2}$$

$$V_t = \frac{k \times T_i}{q} \tag{3}$$

$$I_{cell} = I_{ph} - I_0 \times \left[e^{\left(\frac{V+I_{cell}\times R_S}{\alpha\times V_t}\right)} - 1\right] - \frac{V+I_{cell}\times R_S}{R_{sh}} \tag{4}$$

$$I_{module} = I_{ph} - I_0 \times \left[e^{\left(\frac{V+N_{Scell}I_{module}\times R_S}{\alpha\times V_t\times N_S}\right)} - 1\right] - \frac{V + I_{module} \times N_S \times R_S}{R_{sh}} \tag{5}$$

$$I_{array} = N_P \times I_{ph} - I_0 \times \left[e^{\left(\frac{N_P\times V+N_S I_{array}\times R_S}{\alpha\times V_t\times N_S\times N_P}\right)} - 1\right] - \frac{V \times N_P + I_{array} \times N_S \times R_S}{R_{sh} \times N_P} \tag{6}$$

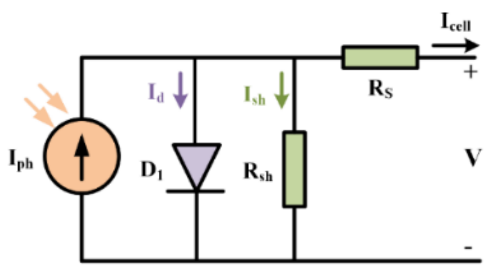

a) PV cell

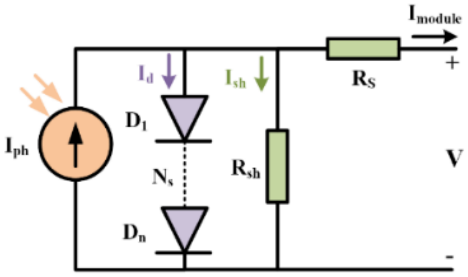

b) PV module

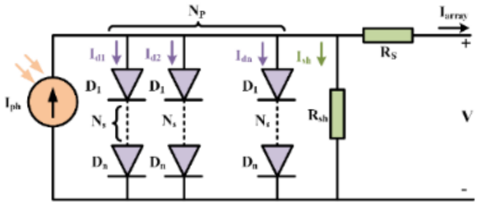

c) PV array

Figure 3. Single diode equivalent circuit model of PV cell, PV module, and PV array

In these equations, q represents the electron charge, k is the Boltzmann constant, and T_i is the junction temperature. The mathematical formulation for the output current (I_{cell}) of the PV cell is given in Equation (4). According to this equation, I_{ph}, the diode ideality factor (α), the reverse saturation current of the diode (I_0), R_{sh}, and R_s are the unknown parameters of this single diode equivalent circuit model. The mathematical expressions for the PV module and array are presented in Equations (5) and (6), respectively. In these equations, I_{module} represents the output current of the PV module, and I_{array} denotes the output current of the PV array. N_S represents the number of series-controlled cells while the N_P denotes the number of parallel-connected modules. A pre-existing photovoltaic model was not employed in this study. The PV arrays were constructed for the required simulations utilizing the mathematical formulae outlined in this discussion. The unknown parameters of the equivalent circuit for the single-diode photovoltaic cell were obtained from the reference mentioned in [55].

2.2 DC-DC Boost converter

The model of the DC-DC boost converter is depicted in Figure 2. Converters are employed to mitigate power and voltage fluctuations in energy sources that are affected by environmental conditions like wind or solar energy. Moreover, the output voltage of the panels may not be sufficient, particularly for fluctuating loads in PV system. Therefore, boost converters are frequently utilized in PV systems. Boost converters ensure that the output voltage of the circuit is higher than the input voltage, depending on the duty cycle of the switching element. The DC-DC boost converter consists of five elements: inductor, capacitor, switching element, diode and load. The values of these components are calculated using Equations (7) -(9).

$$V_0 = \frac{V_i}{1 - d_c} \tag{7}$$

$$L_{min} = \frac{d_c \times (1 - d_c)^2 \times R}{2 \times f_s} \tag{8}$$

$$C_{min} = \frac{d_c}{R \times \frac{\nabla V_0}{V_0} \times f_s} \tag{9}$$

In this context, V_0 denotes the output voltage of the boost converter circuit, V_i represents the input voltage of the same boost converter circuit, L_{min} denotes the minimum value of the inductor, d_c symbolizes the duty cycle, f_s represents the switching frequency, and C_{min} denotes the minimum value of the capacitor.

2.3 Load

Previous studies in the literature on MPPT have shown that a battery pack or ohmic load is connected to the output of the DC-DC boost converter. In this article, an ohmic resistor is preferred as the load.

2.4 MPPT and partial shading

PV cells operate between short circuit current and open circuit voltage on the I-V graph. The current / voltage of a PV cell are not linear. Inside of a PV cell, as the voltage increases up to a certain point, the current also increases. The MPP is the last point just before linearity is disrupted. In order to achieve maximum efficiency, it is important for a PV cell or PV module to function at the specific current and voltage levels that correlate to MPP. Irradiance and temperature are significant factors that affect the efficiency of PV systems. There is a standardized condition for the efficiency analysis of PV systems. This is known as the standard test condition (STC). This standard consists of an irradiance value of 1000W/m2 and an ambient temperature of 25 °C. One of the main factors regarding the efficiency of PV systems is shading. Clouds, buildings, or trees can cause shading. Shade prevents the entire PV system from receiving uniform irradiance. Consequently, the system's efficiency drops significantly. Even if only one cell in a PV system is shaded, the output power of the entire system significantly decreases because the series-connected cells can only produce as much power as the lowest-performing component. To minimize this efficiency loss and continuously operate the PV system at the optimal point, we utilized metaheuristic algorithms to conduct MPPT in this article.

2.5 Evaluation Criteria

To compare the performance of the INFO, EEFO, RTHA, SPBO, and PSO algorithms used to solve the MPPT problem, $MPPT_{efficiency}$ was used as an evaluation criterion. MPPT efficiency is obtained through the calculations provided in Equation (10).

$$MPPT_{efficiency} = \frac{P_{MPP} - P_{MPPalg}}{P_{MPP}} \times 100 \tag{10}$$

In this equation, P_{MPPalg} represents the MPP calculated by the algorithms, and P_{MPP} denotes the system's MPP.

3 INFO algorithm for the MPPT optimization problem under partial shading

In addition to presentation of the INFO algorithm for the MPPT optimization problem under partial shading conditions, brief summaries of the EEFO, RTHA, SPBO, and PSO algorithms are provided in the subsections.

3.1 INFO

INFO algorithm was proposed in 2022 by Ahmadianfar et al. [56]. INFO algorithm is a swarm-based that consists of a series of vectors. It manages the process by calculating the weighted mean of potential solution vectors. INFO algorithm consists of four stages: initialization, updating rule, vector combining, and local search. INFO is based on the weighted mean function shown in Equation (11).

$$WM = \frac{(\sum_{i=1}^{N} x_i \times w_i)}{(\sum_{i=1}^{N} w_i)} \tag{11}$$

In this equation, while weighted mean (WM) is calculated using the weights of the vectors (w_i) with average of positions (x_i). Here N represents the number of vectors. The weights of each vector are computed using Equation (12). According to this equation, ω is the dilation parameter.

$$w = cos(x) \times exp\left(-\frac{x^2}{\omega}\right) \tag{12}$$

3.1.1 Initialization phase

Potential solutions (X), the dimension of the problem (D), and the vector population (N_{INFO}), along with two control parameters, namely, the scaling factor (σ), and the weighted mean factor (δ), are defined at this stage. Subsequently, the vectors are randomly initialized using Equation (13).

$$X_{l,j}^{t} = \{X_{l,1}^{t}, X_{l,2}^{t}, \cdots, X_{l,D}^{t}\} \quad l = 1,2,3,\cdots, N_{INFO} \tag{13}$$

3.1.2 Updating rule

The fundamental principle of this algorithm is not to direct the existing vector to the best solution but to take the average of the vectors. In the INFO algorithm, increasing diversity is the task of this stage. An averaging rule ($MeanRule$) based on the worst, good and the best solution is created at this stage. After initializing the algorithm with a random start, the $MeanRule$ information is used for the next solution. Although it varies based on the objective function, the best solution is selected from among the top five good solutions. The $MeanRule$ is presented in Equation (14).

$$MeanRule = r \times WM1_l^t + (1-r) \times WM2_l^t \quad l = 1,2 \ldots \mathrm{NP} \tag{14}$$

$$WM1_l^t = \delta \times \left[\left(\begin{array}{c} w_3(x_{a2} - x_{a3}) + \\ w_2(x_{a1} - x_{a3}) + \\ w_1(x_{a1} - x_{a2}) \end{array}\right) \Big/ (w_3 + w_2 + w_1 + \varepsilon)\right] + (\varepsilon \times r \tag{14.1}$$

$$w_1 = cos((f(x_{a1}) - f(x_{a2})) + \pi) \times exp(-|(f(x_{a1}) - f(x_{a2}))/\omega|) \tag{14.2}$$

$$w_2 = cos((f(x_{a1}) - f(x_{a3})) + \pi) \times exp(-|(f(x_{a1}) - f(x_{a3}))/\omega|) \tag{14.3}$$

$$w_3 = cos((f(x_{a2}) - f(x_{a3})) + \pi) \times exp(-|(f(x_{a2}) - f(x_{a3}))/\omega|) \tag{14.4.}$$

$$\omega = max(f(x_{a1}),\ f(x_{a2}),\ f(x_{a3})) \tag{14.5}$$

$$WM2_l^t = \delta \times \left[\left(\begin{array}{c} w_3(x_{bs} - x_{bt}) + \\ w_2(x_{bs} - x_{ws}) + \\ w_3(x_{bt} - x_{ws}) \end{array}\right) \Big/ (w_3 + w_2 + w_1 + \varepsilon)\right] + (\varepsilon \times r \tag{14.6}$$

$$\mathrm{w_1 = cos(\,(f(x_{bs}) - f(x_{bt})) + \pi) \times exp(-|(f(x_{bs}) - f(x_{bt}))/\omega|)} \tag{14.7}$$

$$\mathrm{w_2 = cos(\,(f(x_{bs}) - f(x_{ws})) + \pi) \times exp(-|(f(x_{bs}) - f(x_{ws}))/\omega|)} \tag{14.8}$$

$$w_3 = cos(\,(f(x_{bt}) - f(x_{ws})) + \pi) \times exp(-|(f(x_{bt}) - f(x_{ws}))/\omega|) \tag{14.9}$$

$$\omega = f(x_{ws}) \tag{14.10}$$

The first weighted mean ($WM1_l^t$) and the second weighted mean ($\mathrm{WM2}_l^t$) in the $MeanRule$ equations are given in Equation (14.1) and (14.6). In these equations, (w_1), (w_2), and (w_3) represent the first, second, and third wavelet functions, respectively. Wavelet functions are used to compute the weighted mean of vectors. The wavelet functions for the first weighted mean are provided in Equations (14.2) -(14.4), and for the second weighted mean in Equations (14.7) -(14.9). In these equations, w is the dilation parameter, $f(x)$ is the objective function, $a_1, a_{2,}$ and a_3 are unequal integers selected from the range $[1, N_{INFO}]$, ε is a very small number, x_{a1}, x_{a2}, and x_{a3} are the positions of the vectors, $\mathrm{x_{ws}}$, $\mathrm{x_{bt}}$, and $\mathrm{x_{bs}}$ are the worst, good and best solutions, respectively, r is a random number in the range [0,0.5]. In equation (16), the scaling factor (δ) is given. The value of β, which is computed based on an exponential function with the current iteration (t), and the maximum iteration ($\mathrm{T_{INFO}}$), is presented in Equation (15).

$$\beta = \alpha = 2 \times exp\left(-4 \times \frac{t}{T_{INFO}}\right) \tag{15}$$

$$\delta = 2 \times \beta \times rand - \beta \tag{16}$$

After completing the first task of the update rule (calculating the weighted mean), the second task of accelerating convergence begins. This task affects the algorithm's performance and goal to achieve the best result. In Equation (18), this stage varying the step size so that to direct the vectors towards a better direction. The newly obtained vector (z_l^t) is given in Equation (17). Update rule ($Rule_{ur}$) is given Equation (19). In accordance with the r parameter, the new vector update rule is applied to the first and second vectors. In Equation (20), the scaling factor (σ) for the vectors is given and this parameter is related to exploitation and exploration the calculation of α is presented in Equation (21). There, d and c are constant number and equal to 4 and 2, separately.

$$z_l^t = x_l^t + \sigma \times MeanRule + CA \tag{17}$$

$$CA = \begin{cases} randn \times \left(\dfrac{x_{bs} - x_{a1}^t}{f(x_{bs}) - f(x_{a1}^t) + 1} \right) \\ randn \times \left(\dfrac{x_{a2}^t - x_{a3}^t}{f(x_{a2}^t) - f(x_{a3}^t) + 1} \right) \\ randn \times \left(\dfrac{x_{a1}^t - x_{a2}^t}{f(x_{a1}^t) - f(x_{a2}^t) + 1} \right) \end{cases} \tag{18}$$

$$Rule_{ur} = \begin{cases} z1_l^t = x_l^t + \sigma \times MeanRule + \left[\begin{pmatrix} x_{bs} \\ -x_{a1}^t \end{pmatrix} \middle/ \left(\begin{matrix} f(x_{bs}) \\ -f(x_{a1}^t) + 1 \end{matrix} \right. \right. \\ z1_l^t = x_a^t + \sigma \times MeanRule + \left[\begin{pmatrix} x_{a2}^t \\ -x_{a3}^t \end{pmatrix} \middle/ \left(\begin{matrix} f(x_{a2}^t) \\ -f(x_{a3}^t) + 1 \end{matrix} \right. \right. \\ z2_l^t = x_{bs} + \sigma \times MeanRule + \left[\begin{pmatrix} x_{a1}^t \\ -x_b^t \end{pmatrix} \middle/ \left(\begin{matrix} f(x_{a1}^t) \\ -f(x_{a2}^t) + 1 \end{matrix} \right. \right. \\ z2_l^t = x_{bt} + \sigma \times MeanRule + \left[\begin{pmatrix} x_{a1}^t \\ -x_{a2}^t \end{pmatrix} \middle/ \left(\begin{matrix} f(x_{a1}^t) \\ -f(x_{a2}^t) + \end{matrix} \right. \right. \end{cases} \tag{19}$$

$$\sigma = 2 \times \alpha \times rand - \alpha \tag{20}$$

$$\alpha = c \times exp\left(-d \times \frac{t}{T_{INFO}} \right) \tag{21}$$

3.1.3 Vector combining

The third stage's task is to rise population diversity and expand the local search. So, the vectors $z1_l^t$ and $z2_l^t$ are obtained from the update rule operator as seen in Equation (22). The parameter μ is given in Equation (23).

$$Rule_{vc} = \begin{cases} u_l^t = z1_l^t + \mu . |z1_l^t - z2_l^t| & rand_2 < 0.5 \\ u_l^t = z2_l^t + \mu . |z1_l^t - z2_l^t| & rand_2 \geq 0.5 \\ u_l^t = x_l^t & \end{cases} \quad \begin{matrix} rand_1 < 0.5 \\ \\ rand_1 \geq 0.5 \end{matrix} \tag{22}$$

$$\mu = 0.05 \times randn \tag{23}$$

3.1.4 Local search

The fourth stage of this algorithm is the local search. The role of this stage is to support exploitation phase. It achieves this by creating a new vector using mean rule and global position (x_{best}^t). Thus, it tries to reach the global optimum point. The mean rule and global position (x_{best}^t) generate a new vector. In Equations (24)-(28), The update rule ($Rule_{lc}$), the average solution (x_{avg}), and the new solution (x_{rnd}), are given.

$$Rule_{lc} = \begin{cases} u_l^t = x_{bs} + randn \times (MeanRule + \\ \quad randn \times (x_{bs}^t - x_{a1}^t)),\ rand_2 < 0.5 \\ u_l^t = x_{rnd} + randn \times (MeanRule + \\ randn \times (v_1 \times x_{bs} - v_2 \times x_{rnd})),\ rand_2 \geq 0.5 \end{cases} \tag{24}$$

$$x_{avg} = (x_a + x_b + x_3)/3 \tag{25}$$

$$x_{rnd} = \phi \times x_{avg} + (1 - \phi) \times (\phi \times x_{bt} + (1 - \phi) \times x_{bs}) \tag{26}$$

$$v_1 = \begin{cases} 1 & p \leq 0.5 \\ 2 \times rand & p > 0.5 \end{cases} \tag{27}$$

$$v_2 = \begin{cases} rand & p < 0.5 \\ 1 & p \geq 0.5 \end{cases} \tag{28}$$

In Figure 4, flowchart of the INFO algorithm is presented.

3.2 Brief summaries of EEFO, RTHA, SPBO and PSO algorithms

The sources of inspiration, rules/phases/stages/operators that govern their processes, and control parameters of the EEFO, RTHA, SPBO, and PSO algorithms, which are compared with the results of the INFO algorithm, are provided in Table 2 and summarized in the subsections.

3.2.1 EEFO

The EEFO algorithm was proposed in 2024 by Zhao et al. [57]. It is a bio-inspired, swarm-based algorithm. The EEFO algorithm was enhanced according to the foraging behavior of a group of electric eels in nature. EEFO consists of four stages: interaction, resting, hunting, and migration. These stages are designed to ensure exploration and exploitation, which are present in every algorithm. Additionally, the EEFO algorithm includes an energy factor to manage the balance between exploration and exploitation in the search space. The EEFO algorithm has two control parameters: the maximum number of iterations (T_{EEFO}) and the population size (N_{EEFO}). In this study, these values were set to 30 and 4, respectively.

3.2.2 RTHA

The RTHA algorithm was proposed in 2023 by Ferahtia et al [58]. It is a bio-inspired, swarm-based algorithm. RTHA algorithm was developed based on the hunting tactics of the red-tailed hawk. RTHA consists of three phases. These are high soaring, low soaring and stooping, and swooping. In the first phase, the algorithm creates the search space and marks the location where the prey is found. In the second phase, the algorithm models the red-tailed hawk's movement around the prey to select the optimal position to capture it. The final stage models the hawk capturing and striking the prey. RTHA has five control parameters, namely, angle gain (A), the initial value of the radius during low soaring (R_0), control gain (r), maximum number of iterations (T_{RTHA}) and population size (N_{RTHA}). In this article, the parameters A, R_0, and r are set to 15, 0.5, and 1.5, respectively, as in the reference paper [58].

3.2.3 SPBO

The SPBO algorithm was proposed in 2020 by Das et al. [59]. SPBO is a metaheuristic algorithm inspired by the psychology of students striving to become the best in their class. This algorithm categorizes students into four categories: best student, good student, average student, and students who try to improve randomly. This algorithm has two control parameters. These are the maximum number of iterations (T_{SPBO}) and the population size (N_{SPBO}). In this study, control parameters were set to 30 and 4, respectively.

3.2.4 PSO

The PSO algorithm was proposed in 1995 by Eberhart et al. [60]. PSO is inspired by the behavior of animals such as birds, fish, and insects that move in swarms. The core of PSO is based on the exchange of information among particles. The main goal of the PSO algorithm is to ensure that the particles reach the best position in the search space. In the PSO algorithm, all particles in the swarm record the best position they have visited. Before moving again, the entire swarm communicates so that the best position found so far can be shared with other particles. In PSO, the position of the particles depends on their velocity. This algorithm has five control parameters: cognitive component (c_1), social component (c_2), inertia weight (w), maximum number of iterations (T_{PSO}) and population size

(N_{PSO}). The control parameters c_1, c_2, W_{max} and W_{min} of the PSO algorithm have been tested multiple times, and the values provided in the table have been selected through a trial-and-error approach. In this study, cognitive component was set to 1.1, social component to 1.9, the maximum number of iterations to 30, and the population size to 4.

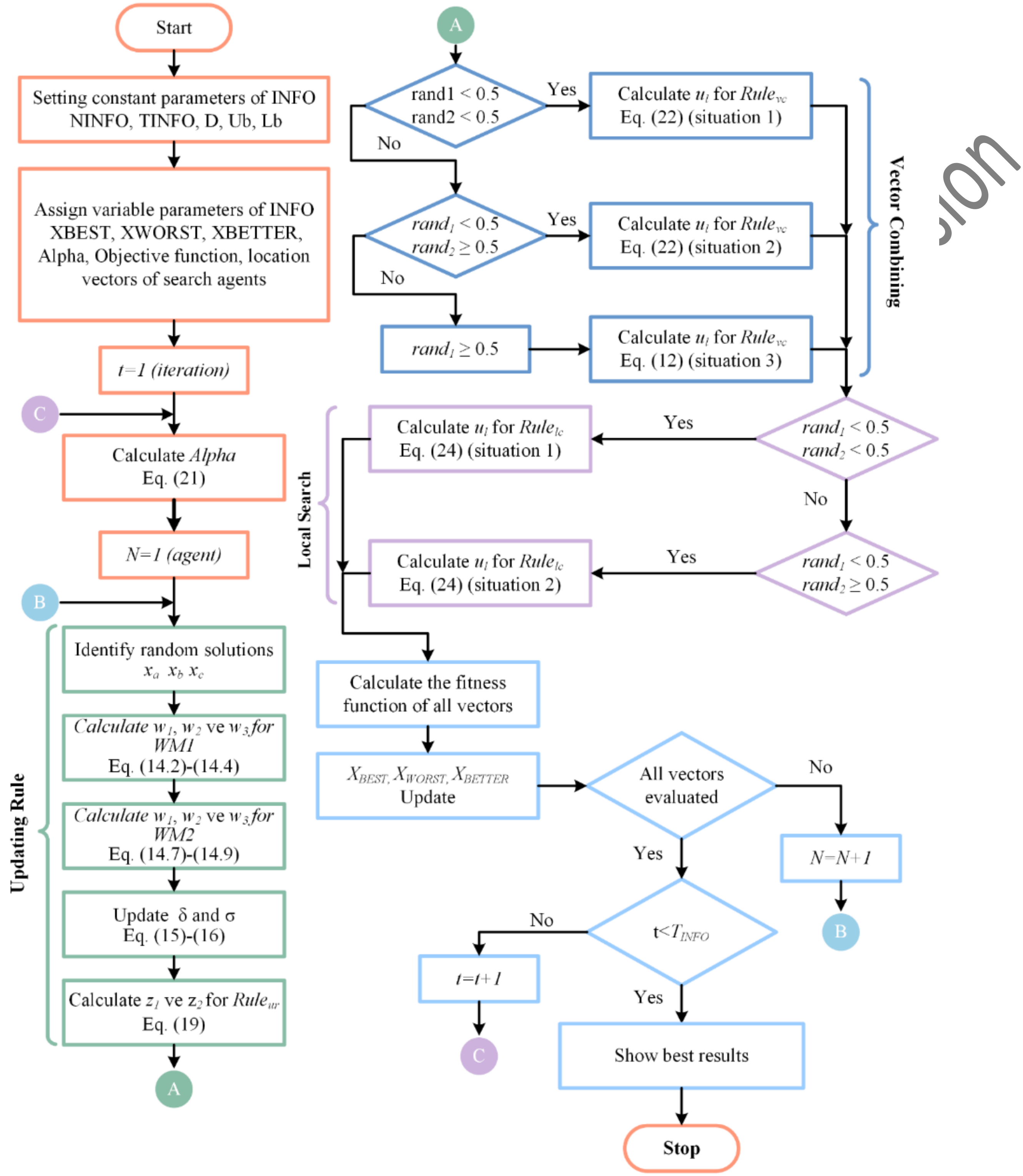

Figure 4. Flow diagram of the INFO algorithm

Table 3. Brief summary of INFO, EEFO, RTHA, SPBO, and PSO algorithms

Algorithm	Inspiration	Rule/Phase/Stage/Operator	Control Parameter	Value
INFO	Weighted mean of vectors	• Updating rule	c	2
		• Vector combining	d	4

		• Local search		
EEFO	Electric eels	• Interaction • Resting • Hunting • Migration	N_{EEFO} T_{EEFO}	4 30
RTHA	Red-tailed hawks	• High soaring • Low soaring • Stooping • Swooping	A R_0 r N_{RTHA} T_{RTHA}	15 0.5 1.5 4 30
SPBO	Student psychology	• Best student • Good student • Average student • Students who improves randomly	N_{SPBO} T_{SPBO}	4 30
PSO	Swarming insects and animals	• Position phase • Velocity phase	c_1 c_2 w_{Max} w_{Min} N_{PSO} T_{PSO}	1.1 1.9 0.8 0.4 4 30

4 Simulation results and analysis

The simulation results and analysis related to solving the MPPT optimization problem are presented in seven subsections: computer specifications, definition of PV system input parameters, definition of INFO, EEFO, RTHA, SPBO, and PSO algorithms' control parameters, MPPT scenarios, results of MPPT optimization, MPPT optimization results based on evaluation metrics, and MPPT optimization results based on statistical tests.

4.1 Computer specifications

For MPPT optimization problem, the PV system was designed using MATLAB/Simulink software. The computer used to solve this problem has the following specifications: Intel® Core i5 processor, 4.4 GHz processor speed, and 16 GB RAM.

4.2 Definition of PV system input parameters

The input parameters of the PV system components, consisting of a PV module, DC-DC boost converter, and load for MPPT optimization, are given in Table 3. The Schutten Solar STM6-40/36 was selected as the PV module. A ready-made block was not used for this module; instead, it was defined using mathematical equations. The parameter values of the created PV module are provided in Table 3. Three PV modules were connected in series, and these series modules were connected in parallel to form three parallel structures. Thus, the simulation studies were conducted with a 3-series 3-parallel (3S3P) configuration. Bypass diodes were added in parallel with each array. In the PV system, the DC-DC boost converter circuit is used to eliminate fluctuations in the output voltage and to change the duty cycle of the PV system. The duty cycle (d_c) is transmitted to the system via the switching element. d_c holding time sent by all algorithms to the Simulink environment was set to D_s 100 ms to prevent voltage fluctuations in the simulation. An ohmic resistor was preferred as the load, and the value of the used resistor is 100 Ω.

Table 4. Parameters of PV system

Component	Parameter	Value	Unit
PV module	PV brand	Schutten Solar STM6-40/36	-
	PV-type	Mono-crystalline	-
	Maximum power (P_{max})	40	W
	Open circuit voltage (V_{oc})	21.6	V
	Short circuit current (I_{sc})	2.36	A
	I_{ph}	1.6639	A
	I_0	1.73866	μA
	α	1.5203	-
	R_{sh}	15.9283	Ω
	R_s	0.00427	Ω
Boost converter	Switching device	IGBT	-
	L	1.2	mH
	C	47	μF
	f_s	20	kHz
	D_s	100	ms
Load	R	100	Ω

4.3 Definition of INFO, EEFO, RTHA, SPBO, and PSO algorithms control parameters

In this article, INFO, EEFO, RTHA, SPBO, and PSO optimization algorithms were used, and in Table 2, the control parameters of these algorithms are provided. INFO has two control parameters, EEFO has 2, RTHA has 5, SPBO has 2, and PSO has five control parameters.

4.4 MPPT scenarios

For MPPT, four different shading scenarios were planned: STC, shading 1, shading 2, and shading 3. The performance of our algorithms solving the MPPT problem was tested with these scenarios. The GMPP value, GMPP location, and irradiance information for these scenarios are provided in Table 4, and the P-V graphs are shown in Figure 4.

- **STC:** All PV modules operate under an irradiance of 1000 W/m² and a temperature of 25 °C. The graphical representation of the STC scenario is shown in Figure 5(a). In this scenario, since there is no shading, a single GMPP point is formed on the P-V graph, and the value of this point, i.e., the maximum power output (P_{max}), is approximately 370 W.
- **Shading 1:** In this shading model, not all PV modules receive equal irradiance. The graphical representation of the Shading 1 scenario is shown in Figure 5(b). The

parallel-connected series PV modules operate at irradiance values of 200 W/m^2, 800 W/m^2, and 300 W/m^2, respectively. In the P-V graph, three different peaks are formed. One of these peaks is the GMPP point, while the other two are LMPP points. In this shading model, the GMPP point is the leftmost of the three peaks on the P-V graph. The maximum power output of this model is approximately 90 W.

- **Shading 2:** In this shading model, the parallel-connected series PV modules operate at irradiance values of 1000 W/m^2, 400 W/m^2, and 800 W/m^2, respectively. The graphical representation of the Shading 2 scenario is shown in Figure 5(c). On the P-V graph, the GMPP point is located in the middle of the three peaks. The maximum power output of this shading model is approximately 200 W.
- **Shading 3:** In this shading model, the parallel-connected series PV modules operate at irradiance values of 850 W/m^2, 700 W/m^2, and 550 W/m^2, respectively. The graphical representation of the Shading 3 scenario is shown in Figure 5(d). On the P-V graph, the GMPP point is located at the rightmost of the three peaks. The maximum power output of this shading model is approximately 215 W.

In the created scenarios, the location of the GMPP point on the P-V graph was set to the right, center, and left. Additionally, in these scenarios, LMPP and GMPP points were chosen to be close to each other to examine the performance of the algorithms under challenging shading conditions.

Table 5. MPPT scenarios

Scenario	Irradiance (W/m²)	Power at GMPP (W)	GMPP Location
STC	$\begin{bmatrix} P/S & S1 & S2 & S3 \\ P1 & 1 & 1 & 1 \\ P2 & 1 & 1 & 1 \\ P3 & 1 & 1 & 1 \end{bmatrix}$	370.5955	STC
Shading 1	$\begin{bmatrix} P/S & S1 & S2 & S3 \\ P1 & 200 & 800 & 300 \\ P2 & 200 & 800 & 300 \\ P3 & 200 & 800 & 300 \end{bmatrix}$	89.9953	Left
Shading 2	$\begin{bmatrix} P/S & S1 & S2 & S3 \\ P1 & 1000 & 400 & 800 \\ P2 & 1000 & 400 & 800 \\ P3 & 1000 & 400 & 800 \end{bmatrix}$	202.4634	Middle
Shading 3	$\begin{bmatrix} P/S & S1 & S2 & S3 \\ P1 & 850 & 700 & 550 \\ P2 & 850 & 700 & 550 \\ P3 & 850 & 700 & 500 \end{bmatrix}$	215.8228	Right

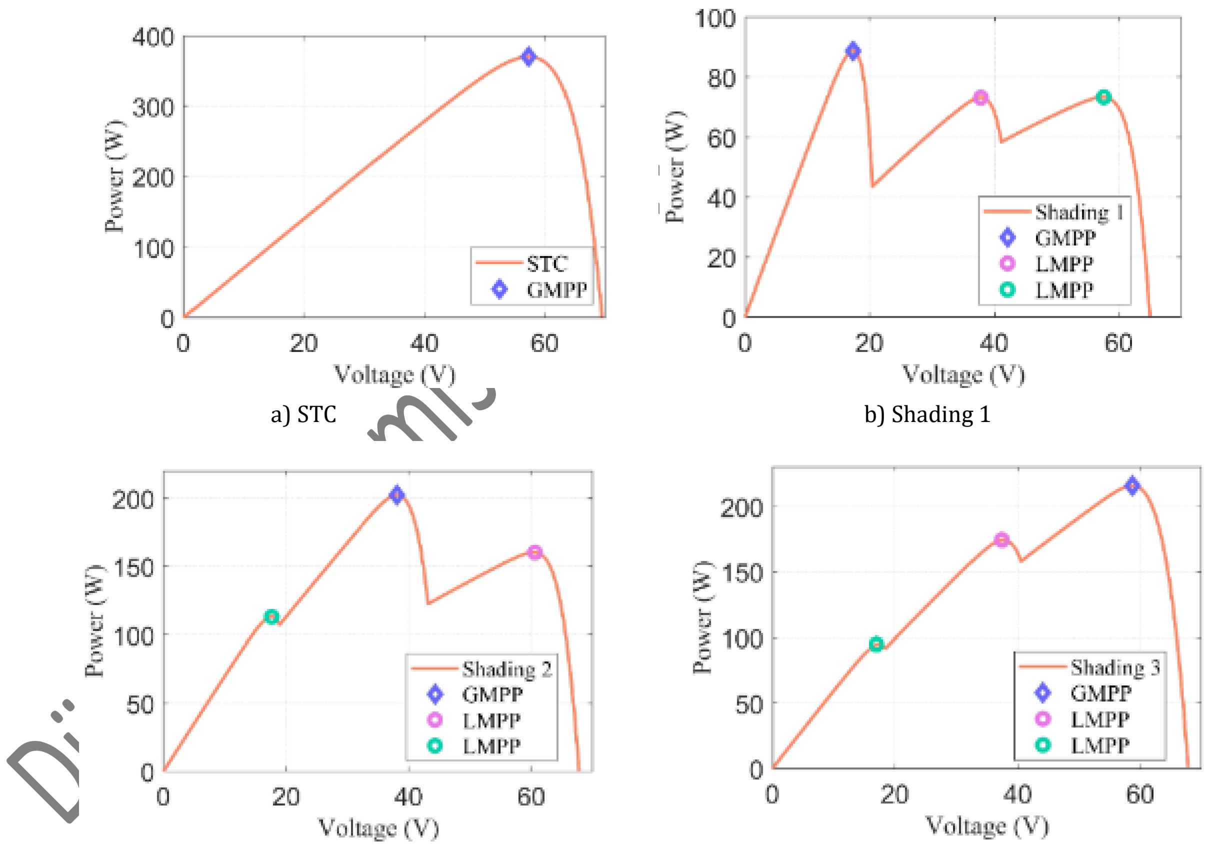

a) STC
b) Shading 1
c) Shading 2
d) Shading 3

Figure 5. P-V curves of partial shading.

4.5 Results of MPPT optimization

The STC, shading 1, shading 2, and shading 3 scenarios were sequentially applied to the designed PV system. The MPPT results of the INFO, EEFO, RTHA, SPBO, and PSO algorithms were recorded, and their performance was evaluated using the MPPT efficiency given in Equation (10).

4.5.1 Results of scenario: STC

STC is the test condition where there is no shading, meaning there is optimal irradiance and temperature. The simulation results of the INFO, EEFO, RTHA, SPBO, and PSO algorithms under these conditions are provided in Table 5. This table includes the following information: P_{MPP} (W), P_{MPPalg} (W), MPP tracking time (s), MPPT efficiency (%), and MPPT efficiency rank. The results in the table are the best results obtained from 30 independent runs of each algorithm. Upon examining the Table 5, it can be seen that all algorithms achieved over 99% MPPT efficiency. Additionally, when ranked by MPPT efficiency, the INFO algorithm is the most successful. Figure 6 presents the P-V graphs of all algorithms run under STC conditions. Upon examining the graphs, it is evident that all algorithms successfully found the MPP point, indicating that all algorithms are usable under STC conditions.

4.5.2 Results of scenario: Shading 1

Shading 1 is a scenario model where shading occurs, and the GMPP is located on the left side. Under this scenario, the P_{MPP} (W), P_{MPPalg} (W), MPP tracking time (s), MPPT efficiency (%), and MPPT efficiency rank of the INFO, EEFO, RTHA, SPBO, and PSO algorithms are provided in Table 6. The results in the table 6 are the best results obtained from 30 independent runs of each algorithm. When examining the results, it can be seen that all algorithms achieved over 98% MPPT efficiency. When ranked by MPPT efficiency, the INFO algorithm is the most successful. Figure 7 presents the P-V graphs of all algorithms run under shading 1 conditions. Upon examining the graphs, it is evident that all algorithms successfully found the GMPP point, indicating that the algorithms are usable in this scenario model.

4.5.3 Results of scenario: Shading 2

Shading 2 is a scenario model where shading occurs, and the GMPP is located in the middle of the three peaks formed. Under this scenario, the P_{MPP} (W), P_{MPPalg} (W), MPP tracking time (s), MPPT efficiency (%), and MPPT efficiency rank of the INFO, EEFO, RTHA, SPBO, and PSO algorithms are provided in Table 7. The results in the table are the best results obtained from 30 runs of each algorithm. When examining the results, it can be seen that all algorithms achieved over 99% MPPT efficiency. When ranked by MPPT efficiency, the INFO algorithm is the most successful. Figure 8 presents the P-V graphs of all algorithms run under shading 2 conditions. Upon examining the graphs, it is evident that all algorithms successfully found the GMPP point, indicating that the algorithms are usable in this scenario model.

4.5.4 Results of scenario: Shading 3

Shading 3 is a scenario model where shading occurs, and the GMPP is located on the right side. Under this scenario, the P_{MPP} (W), P_{MPPalg} (W), MPP tracking time (s), MPPT efficiency (%), and MPPT efficiency rank of the INFO, EEFO, RTHA, SPBO, and PSO algorithms are provided in Table 8. The results in the table 8 are the best results obtained from 30 independent runs of each algorithm. When examining the results, it can be seen that all algorithms achieved over 99% MPPT efficiency. When ranked by MPPT efficiency, the INFO algorithm is the most successful. Figure 9 presents the P-V graphs of all algorithms run under shading 3 conditions. Upon examining the graphs, it is evident that all algorithms successfully found the GMPP point, indicating that the algorithms are usable in this scenario model.

Table 6. Results of MPPT optimization scenario: STC

Algorithm	P_{MPP} (W)	P_{MPPalg} (W)	MPP Tracking Time (s)	MPPT Efficiency (%)	MPPT Efficiency Rank
INFO	370.5954	370.294395687	0.141554535	99.918751223	1
EEFO	370.5954	370.204100199	0.581360925	99.894386251	5
RTHA	370.5954	370.293337734	0.144730806	99.918465749	2
SPBO	370.5954	370.286416007	0.141255258	99.916598018	3
PSO	370.5954	370.279889272	0.134185720	99.914836870	4

Table 7. Results of MPPT optimization scenario: Shading 1

Algorithm	P_{MPP} (W)	P_{MPPalg} (W)	MPP Tracking Time (s)	MPPT Efficiency (%)	MPPT Efficiency Rank
INFO	89.9953	88.678347477	0.131130323	98.536626025	1
EEFO	89.9953	88.675386103	0.231645710	98.533335438	5
RTHA	89.9953	88.669446464	0.560735668	98.526735496	3
SPBO	89.9953	88.678274249	0.188122822	98.536544657	2
PSO	89.9953	88.677785309	0.280607540	98.536001362	4

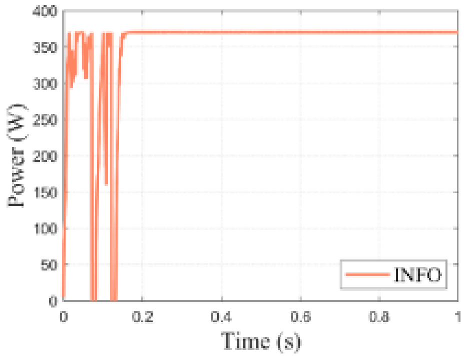

a) INFO

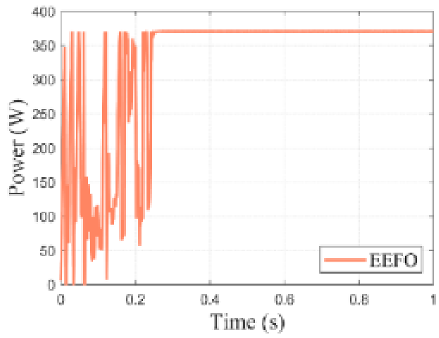

b) EEFO

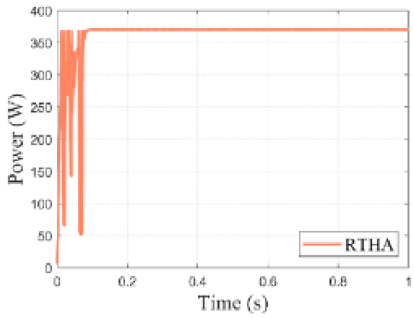

c) RTHA

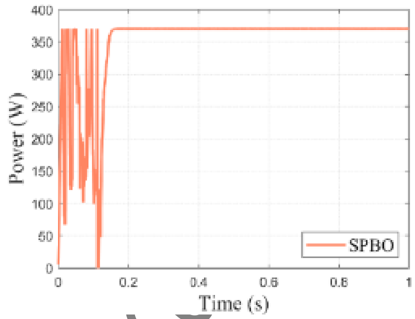

d) SPBO

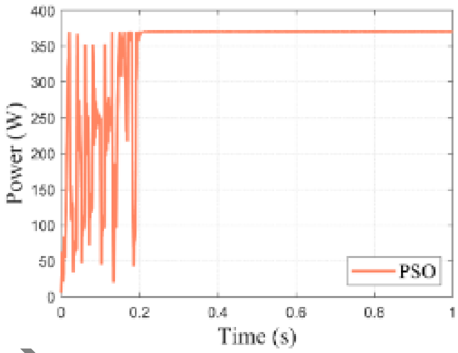

e) PSO

Figure 6. Results of STC power- time graph

Table 8. Results of MPPT optimization scenario: shading 2

Algorithm	P_{MPP} (W)	P_{MPPalg} (W)	MPP Tracking Time (s)	MPPT Efficiency (%)	MPPT Efficiency Rank
INFO	202.4634	202.460432218	0.238326224	99.998522782	1
EEFO	202.4634	202.459966503	0.335683211	99.998292757	2
RTHA	202.4634	202.407728662	0.149314755	99.972491632	4
SPBO	202.4634	202.459550753	0.240279532	99.998087412	3
PSO	202.4634	202.403081026	0.238231818	99.970196089	5

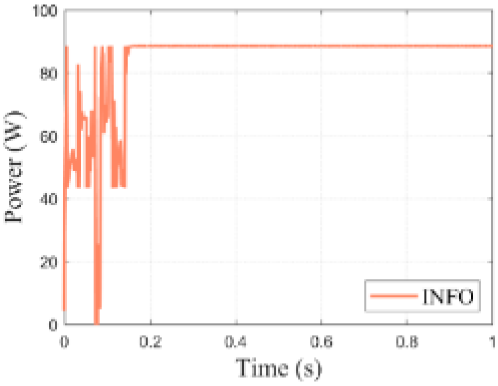

a) INFO

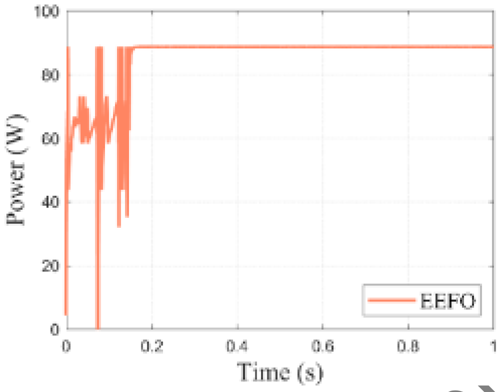

b) EEFO

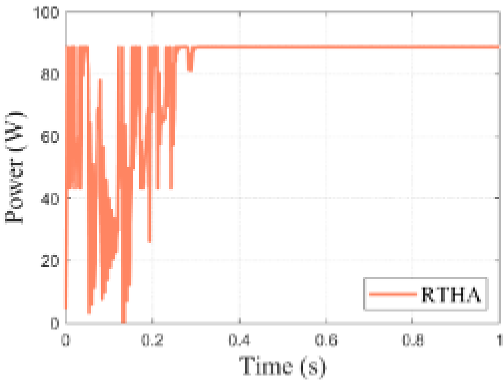

c) RTHA

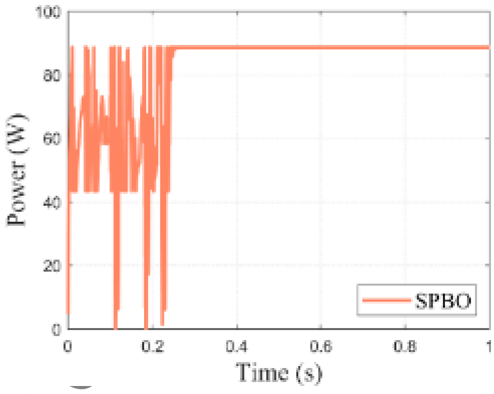

d) SPBO

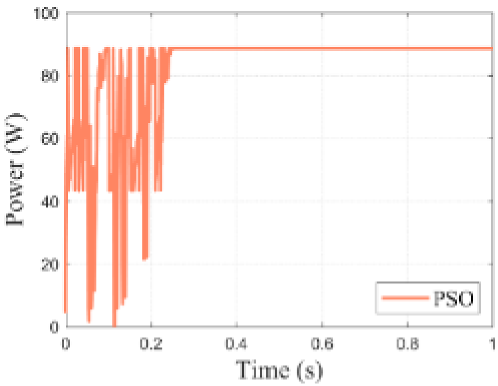

e) PSO

Figure 7. Results of shading 1 power-time graph

Table 9. Results of MPPT optimization scenario: shading 3

Algorithm	P_{MPP} (W)	P_{MPPalg} (W)	MPP Tracking Time (s)	MPPT Efficiency (%)	MPPT Efficiency Rank
INFO	215.8228	215.793319619	0.443408974	99.986332950	1
EEFO	215.8228	215.783301603	0.184012194	99.981691172	2
RTHA	215.8228	215.759109543	0.242454338	99.970481950	4
SPBO	215.8228	215.751963737	0.235139757	99.967170990	5
PSO	215.8228	215.768350699	0.429528723	99.974763775	3

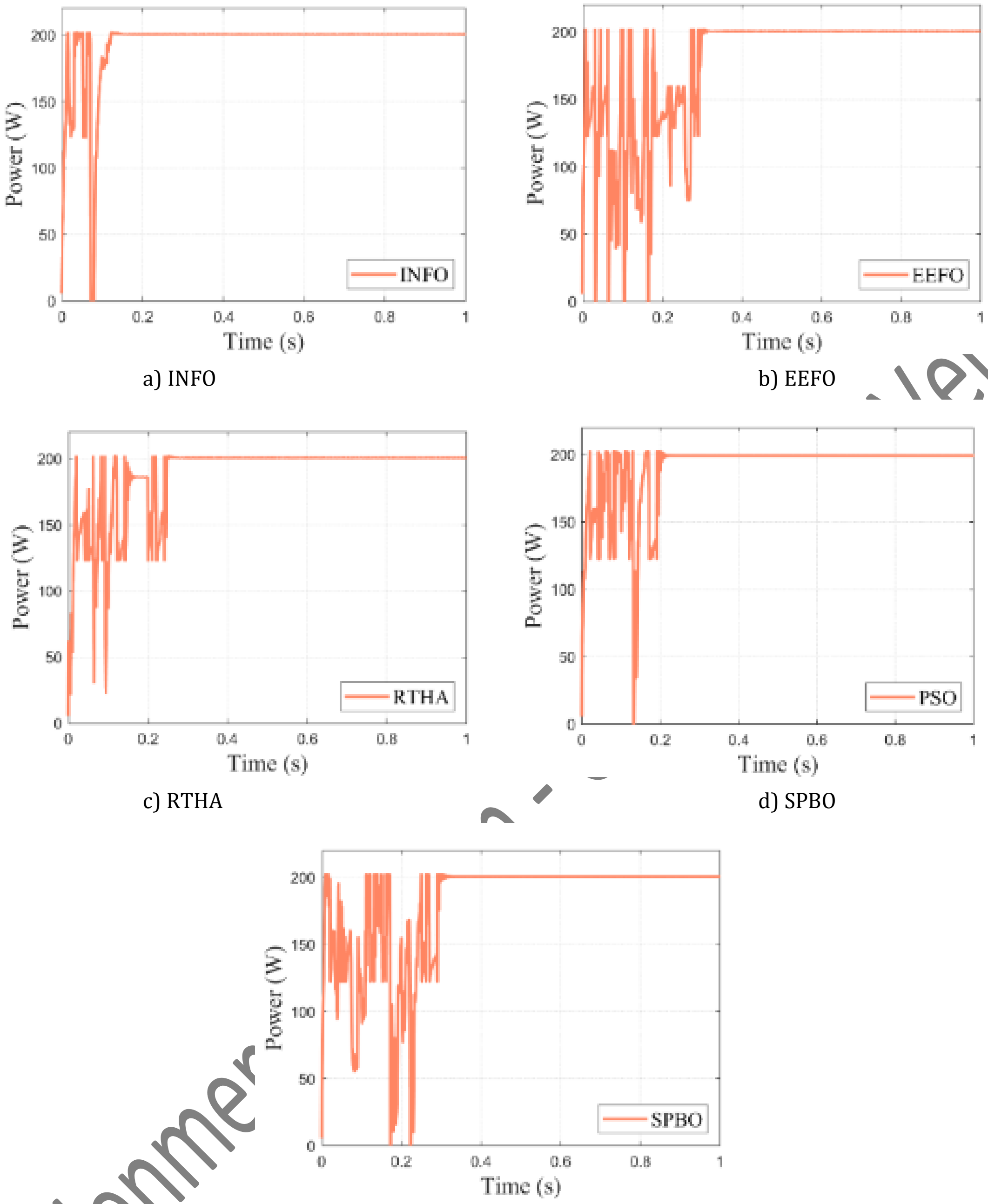

a) INFO b) EEFO

c) RTHA d) SPBO

e) PSO

Figure 8. Results of shading 2 power- time graph

4.6 Results of MPPT optimization

In order to optimize MPPT, all scenarios were run 30 times independently with our algorithms, and the results were recorded. The recorded findings were assessed with respect to computational accuracy and computational time using the evaluation metrics.

4.6.1 Computational accuracy

Performance of the algorithms for all scenarios over 30 runs was evaluated in terms of computational accuracy (P_{MPPalg}), and the results are demonstrated in Table 9. A general inspection is provided at the bottom of the table to facilitate the evaluation of the results. The results of the algorithms were analyzed using the evaluation metrics of minimum, mean, maximum, standard deviation. Since MPPT optimization is a maximization problem, all metrics except for the standard deviation are ranked from largest to smallest. In this table, a rank of 1 represents the most successful algorithm, while a rank of 5 represents the least successful algorithm. When examining the total ranking, which is assessed based on the average ranking for all metrics, it was observed that the INFO algorithm is the most successful. According to both individual and overall results, the solutions produced by the INFO algorithm are more consistent and successful than the other algorithms.

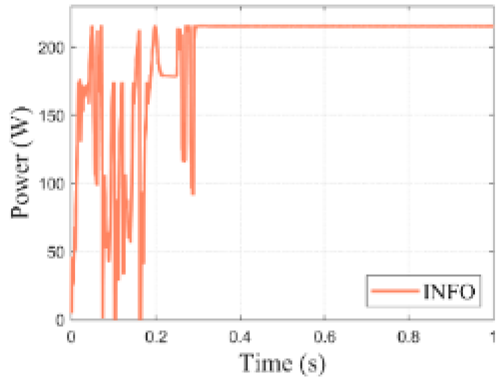

a) INFO

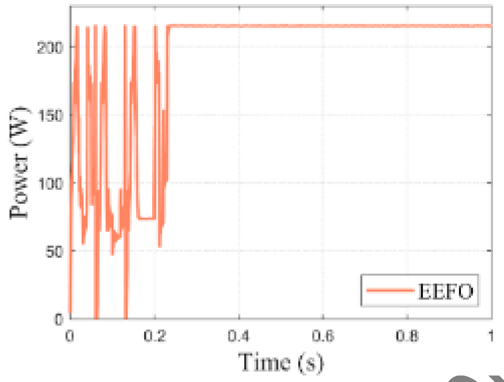

b) EEFO

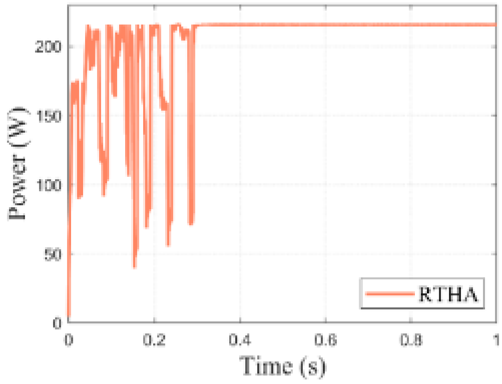

c) RTHA

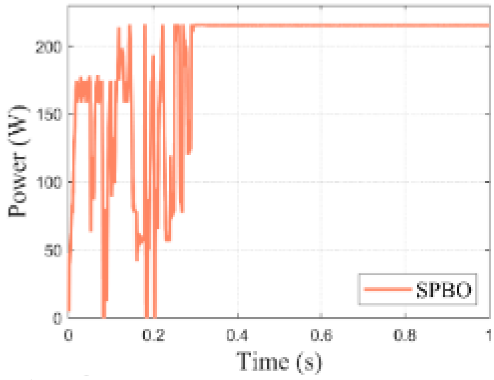

d) SPBO

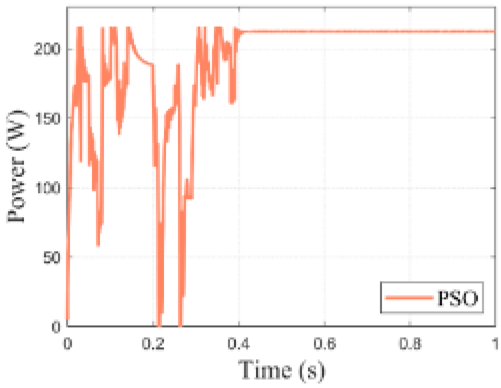

e) PSO

Figure 9. Results of shading 3 power- time graph.

4.6.2 Computational time

The computational complexity of the INFO, EEFO, RTHA, SPBO, and PSO algorithms employed in this study depends on the maximum number of iterations (T_{INFO}, T_{EEFO}, T_{RTHA}, T_{SPBO}, T_{PSO}) the population size (N_{INFO}, N_{EEFO}, N_{RTHA}, N_{SPBO}, N_{PSO}) and the problem dimension (d). The computational complexity formulas for these algorithms are given in Equations 28–32, respectively.

$$O(INFO) = O(T_{INFO} \times N_{HOA} \times d) \quad (28)$$

$$O(EEFO) = O(T_{EEFO} \times N_{EEFO} \times d) \quad (29)$$

$$O(RTHA) = O(T_{RTHA} \times N_{RTHA} \times d) \quad (30)$$

$$O(SPBO) = O(T_{SPBO} \times N_{SPBO} \times d) \quad (31)$$

$$O(PSO) = O(T_{PSO} \times N_{PSO} \times d) \quad (32)$$

The performance of these algorithms for all scenarios over 30 runs was evaluated in terms of computational time, and the outcomes are recorded in Table 10. A general inspection is provided at the bottom of the table to facilitate the evaluation of the results. The algorithms' computational time results were analyzed using the evaluation metrics than ranked from smallest to largest. When examining the total ranking, which is assessed based on the average ranking for all metrics, it is stated that the INFO is the fastest algorithm. The algorithms can be ranked based on the standard deviation metric of computational time as INFO, PSO, SPBO, EEFO, and RTHA. The INFO algorithm ranks first in both computational accuracy and computational time. On the other hand, the EEFO algorithm ranks second in computational accuracy (standard deviation metric) but fourth in computational time. It is not entirely correct to evaluate algorithms based solely on computational speed.

Table 10. Computational accuracy (P_{MPPalg}) values for 30 runs

Scenario	Algorithm	Minimum	Rank	Mean	Rank	Maximum	Rank	Standard Deviation	Rank
STC	INFO	97.955024463	1	345.452290862	1	370.294395687	1	65.228535457	1
	EEFO	74.300717390	2	292.694948651	4	370.204100199	5	86.843124322	2
	RTHA	43.280487206	5	306.461347189	3	370.293337734	2	100.862534197	4
	SPBO	73.374961994	3	278.144033516	5	370.286416007	3	101.663011661	5
	PSO	67.138108397	4	309.953248733	2	370.279889272	4	97.891634323	3
Shading 1	INFO	61.907736805	1	79.073770220	1	88.678347477	1	9.403077260	1
	EEFO	46.000277648	4	75.232226322	2	88.675386103	4	12.459007718	4
	RTHA	50.308382767	2	74.594803815	4	88.669446464	5	9.461124980	2
	SPBO	49.649242458	3	73.516421739	5	88.678274249	2	9.809112660	3
	PSO	44.444612666	5	74.726489162	3	88.677785309	3	13.084648658	5
Shading 2	INFO	153.359561825	1	193.456665039	1	202.460432218	1	12.862841063	1
	EEFO	13.360287259	5	159.235791528	5	202.459966503	2	37.579794382	4
	RTHA	62.374604752	4	164.839356348	4	202.407728662	4	41.726370190	5
	SPBO	129.410386798	2	190.937856196	2	202.459550753	3	20.655018495	2
	PSO	69.602866059	3	183.267487513	3	202.403081026	5	29.732151321	3
Shading 3	INFO	78.305977577	1	199.903284278	1	215.793319619	1	31.286826185	1
	EEFO	68.244279253	2	176.347690810	4	215.783301603	2	37.325329256	2
	RTHA	57.601884014	5	175.568794333	5	215.759109543	4	55.921143579	5
	SPBO	57.601884036	4	178.584180192	3	215.751963737	5	48.102392309	4
	PSO	57.601880718	3	184.227942644	2	215.768350699	3	47.283058094	3
Scenario	**Algorithm**	**Mean Rank**	**Total Rank**	**Mean Rank**	**Total Rank**	**Mean Rank**	**Total Rank**	**Mean Rank**	**Total Rank**
STC Shading 1 Shading 2 Shading 3	INFO	1	1	1	1	1	1	1	1
	EEFO	3.25	3	3.75	3	3.25	2	3	2
	RTHA	4	5	4	5	3.75	3	4	5
	SPBO	3	2	3.75	3	3.25	2	3.75	4
	PSO	3.75	4	2.5	2	3.75	3	3.5	3

Table 11. Computational times values for 30 runs

Scenario	Algorithm	Minimum	Rank	Mean	Rank	Maximum	Rank	Standard Deviation	Rank
STC	INFO	0.141554535	4	0.379338996	1	1.130601579	1	0.291374607	1
	EEFO	0.147670937	5	1.056636987	5	1.566972325	2	0.615141584	4
	RTHA	0.090495923	1	0.990388498	4	4.667068048	5	1.341881332	5
	SPBO	0.141255258	3	0.536560457	3	1.567014106	3	0.396103558	2
	PSO	0.130428383	2	0.514153774	2	1.568090278	4	0.470457937	3
Shading 1	INFO	0.112801897	2	0.361952719	3	1.559556248	3	0.267388011	3
	EEFO	0.149143050	5	0.658589255	4	1.561778813	4	0.504764641	4
	RTHA	0.131931967	3	0.742473777	5	4.581600047	5	1.133262503	5
	SPBO	0.147605150	4	0.345967825	2	0.849073878	1	0.175437520	1
	PSO	0.100143525	1	0.332134818	1	1.037585589	2	0.193048506	2
Shading 2	INFO	0.096964729	1	0.243467089	1	0.645670166	1	0.139086438	1
	EEFO	0.147311447	5	0.823075015	5	1.596622325	4	0.457335654	4
	RTHA	0.140906333	4	0.717591982	4	4.395430985	5	0.896026814	5
	SPBO	0.133022947	3	0.313205900	2	1.564238472	2	0.291695234	3
	PSO	0.130365980	2	0.370753535	3	1.564586795	3	0.284002378	2
Shading 3	INFO	0.132006949	3	0.379566887	1	1.483584262	1	0.318474071	1
	EEFO	0.182548994	5	0.827965822	4	1.565018367	2	0.565184573	3
	RTHA	0.120788841	1	1.280649996	5	4.681229484	5	1.683392051	5
	SPBO	0.148153674	4	0.809822232	3	4.629693700	4	0.872586050	4
	PSO	0.126537645	2	0.546406237	2	1.566938549	3	0.422117618	2
Scenario	**Algorithm**	**Mean Rank**	**Total Rank**	**Mean Rank**	**Total Rank**	**Mean Rank**	**Total Rank**	**Mean Rank**	**Total Rank**
STC Shading 1 Shading 2 Shading 3	**INFO**	2.5	3	1.5	**1**	1.5	**1**	1.5	**1**
	EEFO	5	5	4.5	4	3	3	3.75	4
	RTHA	2.25	2	4.5	4	5	5	5	5
	SPBO	3.5	4	2.5	3	2.5	2	2.5	3
	PSO	1.75	**1**	2	2	3	3	2.25	2

The key is the consistency of the algorithms in producing accurate and stable results. Therefore, computational time alone is not a sufficient criterion. Computational time and accuracy should be evaluated based on the problem's objective.

The main goal in solving the MPPT problem under partial shading conditions is to identify the GMPP point accurately. In PV systems, shading conditions do not change constantly; they may vary every few minutes. Thus, computational time can be considered secondary for MPPT.

4.7 MPPT optimization results based on statistical test

The INFO algorithm's MPPT optimization results have been successful and consistent according to evaluation metrics. To further strengthen our confidence in the INFO algorithm's ability to solve this problem, we also subjected it to the Friedman test. Friedman test ranks the performance of all algorithms separately and allows for comparison among the algorithms within the group [61]. The Friedman test checks if there is a meaningful difference between the algorithms and ranks this algorithm according to their significance level [62]. Since the problem of this article is MPPT optimization, a higher Friedman mean rank indicates higher algorithm success. The Friedman test results for the five metaheuristic algorithms, at a 5% significance level, are provided in Table 11. According to the table 11, it can be seen that the P-value is less than 0.05 for all scenarios. This indicates that there is a meaningful difference between the algorithms. Table 12 provides each algorithm's importance rank, mean rank, and total rank across the all of models. This table statistically demonstrates that the INFO algorithm is the most successful.

Table 12. Mean and total ranking of algorithms based on Friedman test.

Scenario	INFO	EEFO	RTHA	SPBO	PSO
STC	**1**	4	3	5	2
Shading 1	**1**	3	4	5	2
Shading 2	**1**	4	3	2	2
Shading 3	**1**	5	2	4	3
Mean Rank	**1**	4	3	4	2.25
Total Rank	**1**	4	3	4	2

Table 13. Ranking list of algorithms according to the Friedman test

Scenario	Algorithm	Friedman Mean Rank	Algorithm Rank	P-value	Conclusion
STC	INFO	4.4333	1	4.3834 E-12	P-value: 4.3834 E-12<0.05
	EEFO	2.0333	4		
	RTHA	3.1333	3		
	SPBO	1.7667	5		
	PSO	3.6333	2		
Shading 1	INFO	4.3000	1	3.8687E-07	P-value: 3.8687E-07<0.05
	EEFO	2.9333	3		
	RTHA	2.8000	4		
	SPBO	1.9000	5		
	PSO	3.0667	2		
Shading 2	INFO	3.9667	1	4.4426E-16	P-value: 4.4426E-16<0.05
	EEFO	1.3667	4		
	RTHA	1.8667	3		
	SPBO	3.9000	2		
	PSO	3.9000	2		
Shading 3	INFO	4.7333	1	1.8802E-11	P-value: 1.8802E-11<0.05
	EEFO	1.8333	5		
	RTHA	3.1000	2		
	SPBO	2.4667	4		
	PSO	2.8667	3		

5 Experimental validation

An experimental study was conducted to evaluate the real-time performance of the INFO algorithm, whose effectiveness had been demonstrated through simulation studies and statistical tests. The physical layout of the experimental setup is presented in Figure 10. The system consists of a Magna-Power programmable PV simulator, 250 W boost type DC-DC converter, resistive load and a microcontroller board based on STM32. During the experiments, a 155 W thin-film PV panel was used. The performance of the INFO algorithm was assessed under two different test scenarios: STC and partial shading conditions.

Test 1 – STC: In the first stage, the system was operated under standard test conditions, specifically 1000 W/m^2 irradiance and 25 °C ambient temperature. Under these stable environmental conditions, the INFO algorithm accurately and rapidly tracked the maximum power point (MPP). In this scenario, the algorithm achieved an efficiency of 99.83%. The corresponding P–V and P–I curves are shown in Figure 11(a) and (b), respectively.

Test 2 – Partial shading condition: In this stage, the performance of the INFO algorithm under challenging environmental conditions was analyzed. For this purpose, a partial shading scenario was created by gradually reducing the irradiance level using the PV simulator in a controlled manner. The INFO algorithm responded promptly to this sudden change, successfully converged to the new maximum power point, and maintained high system efficiency. The efficiency achieved in this scenario was 99.37%. The corresponding P–V and P–I curves are presented in Figure 11(c) and (d), Correspondingly. As clearly seen in Figure 11, the GMPP points are explicitly marked, illustrating the precise tracking capability of the algorithm.

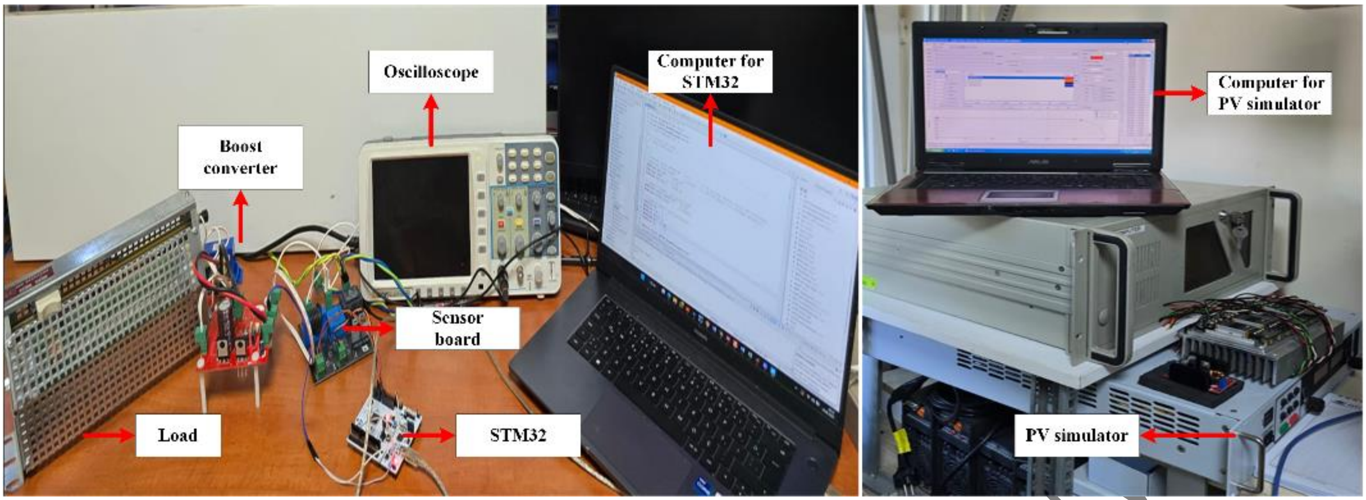

Figure 10. Experimental setup

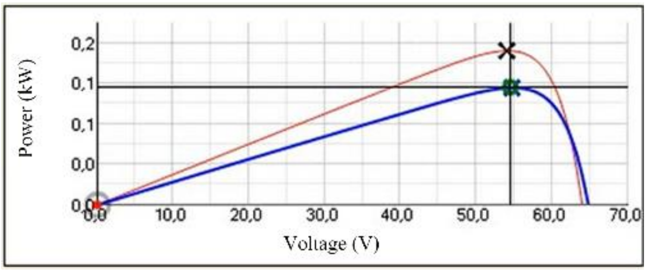

(a) P-V curve at Test 1

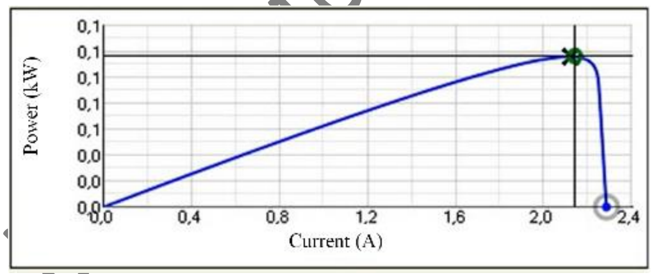

(b) P-I curve at Test 1

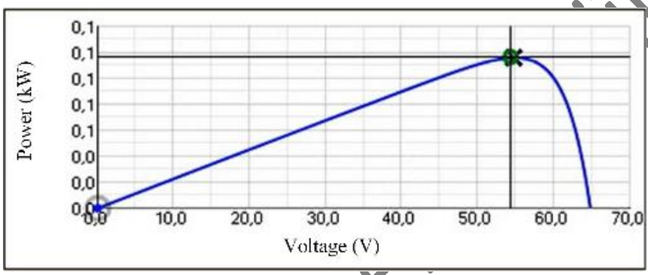

(c) P-V curve at Test 2

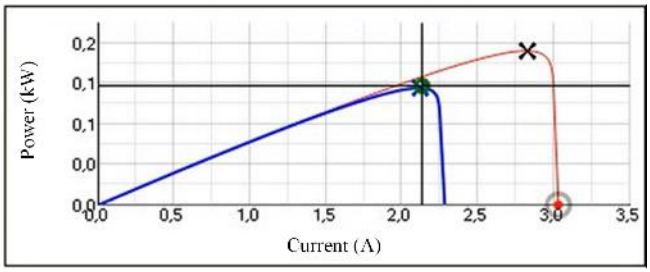

(d) P-I curve at Test 2

Figure 11. Experimental performance of the INFO algorithm: P–V and P–I profiles

6 Conclusion

In this article, the MPPT problem was addressed to accurately and quickly reach the GMP point. The MPPT optimization problem of a PV system operating under partial shading conditions was solved using the INFO, EEFO, RTHA, SPBO, and PSO algorithms. INFO, EEFO, RTHA, and SPBO were utilized for the first time in this article to solve the MPPT optimization problem. The widely used PSO algorithm in the literature was chosen to compare the performance of these new algorithms. The algorithms were tested under challenging shading scenarios where LMPP and GMPP varied. The results of the algorithms were evaluated from two perspectives: evaluation metrics and the Friedman test. The indicated that the INFO algorithm performed more successfully and consistently than its competitors. As demonstrated by both evaluation metrics and the Friedman test, INFO was proven to be faster, more reliable, and more consistent than the EEFO, RTHA, SPBO, and PSO algorithms.

Additionally, an experimental validation was carried out to confirm the real-time applicability and performance of the INFO algorithm. The experimental setup included a programmable PV simulator, a boost converter, and an STM32 microcontroller. The INFO algorithm was embedded on the STM32 board and tested under both ideal and partial shading conditions. The experimental results verified that INFO effectively tracked the maximum power point in real hardware scenarios, demonstrating fast convergence and stable operation, consistent with the simulation outcomes.

In future studies, it is aimed to use the INFO algorithm along with well-known metaheuristic algorithms and newly proposed algorithms for MPPT optimization. It is planned to work on hybrid algorithm structures to further upgrade the performance and success rate of the INFO algorithm.

7 Author contribution statements

Author 1: Conceptualization, Investigation, Methodology, Software, Visualization, Writing—Original Draft, Writing - Review & Editing. Author 2: Conceptualization, Methodology, Supervision, Writing - Review & Editing. Author 3: Conceptualization, Visualization, Supervision, Writing—Original Draft, Writing - Review & Editing. All authors read and approved the final manuscript.

8 Ethics committee approval and conflict of interest statement

There is no need to obtain permission from the ethics committee for the article prepared. There is no conflict of interest with any person or institution in the article prepared.

9 References

[1] Khan K, Su CW, Rehman AU, Ullah R. "Is technological innovation a driver of renewable energy?". *Technology in Society*, 70(102044), 102044, 2022.

[2] Kishore DJK, Mohamed MR, Sudhakar K, Peddakapu K. "Swarm intelligence-based MPPT design for PV systems under diverse partial shading conditions". *Energy*, 265(126366), 126366, 2023.

[3] Olabi AG, Abdelkareem MA. "Renewable energy and climate change". *Renewable and Sustainable Energy Reviews*, 158(112111), 112111, 2022.

[4] Gulzar MM, Iqbal A, Sibtain D, Khalid M. "An innovative converterless solar PV control strategy for a grid connected hybrid PV/wind/fuel-cell system coupled with battery energy storage". *IEEE Access: Practical Innovations, Open Solutions*, 11, 23245–23259,2023.

[5] P Bojek. "Tracking Clean Energy Progress 2023. Available" https://www.iea.org/reports/tracking-clean-energy-progress (01.01.2025).

[6] Sahu A, Yadav N, Sudhakar K. "Floating photovoltaic power plant: A review". *Renewable and Sustainable Energy Reviews*, 66, 815–824, 2016.

[7] Refaat A, Khalifa AE, Elsakka MM, Elhenawy Y, Kalas A, Elfar MH. "A novel metaheuristic MPPT technique based on enhanced autonomous group Particle Swarm Optimization Algorithm to track the GMPP under partial shading conditions - Experimental validation". *Energy Conversion and Management*, 287(117124), 117124, 2023.

[8] Mirza AF, Ling Q, Javed MY, Mansoor M. "Novel MPPT techniques for photovoltaic systems under uniform irradiance and Partial shading". *Solar Energy*, 184, 628–648, 2019.

[9] Yang B, Zhu T, Wang J, Shu H, Yu T, Zhang X, Yao W, Sun L. "Comprehensive overview of maximum power point tracking algorithms of PV systems under partial shading condition". *Journal of Cleaner Production*, 268(121983), 121983, 2020.

[10] Wasim MS, Amjad M, Habib S, Abbasi MA, Bhatti AR, Muyeen SM. "A critical review and performance comparisons of swarm-based optimization algorithms in maximum power point tracking of photovoltaic systems under partial shading conditions". *Energy Reports*, 8, 4871–4898,2022.

[11] Kollimalla SK, Mishra MK. "Variable perturbation size adaptive P&O MPPT algorithm for sudden changes in irradiance". *IEEE Transactions on Sustainable Energy*, 5(3), 718–728, 2014.

[12] Swaminathan N, Lakshminarasamma N, Cao Y. "A fixed zone perturb and observe MPPT technique for a standalone distributed PV system". *IEEE Journal of Emerging and Selected Topics in Power Electronics*, 10(1), 361–374,2021.

[13] Jately V, Azzopardi B, Joshi J, Venkateswaran BV, Sharma A, Arora S. "Experimental Analysis of hill-climbing MPPT algorithms under low irradiance levels". *Renewable and Sustainable Energy Reviews*, 150(111467), 111467, 2021.

[14] Kumar V, Bindal RK. "A comparative analysis of effective MPPT technology for photovoltaic system with boost converter". *Materials Today: Proceedings*, 69, A1–A5, 2022.

[15] Loukriz A, Haddadi M, Messalti S. "Simulation and experimental design of a new advanced variable step size Incremental Conductance MPPT algorithm for PV systems". *ISA Transactions*, 62, 30–38, 2016.

[16] Khan MK, Zafar MH, Riaz T, Mansoor M, Akhtar N. "Enhancing efficient solar energy harvesting: A process-in-loop investigation of MPPT control with a novel stochastic algorithm". *Energy Conversion and Management: X*, 21(100509), 100509, 2024.

[17] Hsu TW, Wu HH, Tsai DL, Wei CL. "Photovoltaic energy harvester with fractional open-circuit voltage based maximum power point tracking circuit". *IEEE Transactions on Circuits and Systems. II, Express Briefs: A Publication of the IEEE Circuits and Systems Society*, 66(2), 257–261, 2019.

[18] Shebani MM, Iqbal T, Quaicoe JE. "Comparing bisection numerical algorithm with fractional short circuit current and open circuit voltage methods for MPPT photovoltaic systems". *2016 IEEE Electrical Power and Energy Conference (EPEC)*, 1–5,2016.

[19] Luo G, Liu J, Yang T, Dou Y, Chen N. "A constant current and constant voltage charging circuit through MPPT method and its stability analysis". *3rd China International SAR Symposium (CISS)*, 1–6, 2022.

[20] Motahhir S, El Hammoumi A, El Ghzizal A. "The most used MPPT algorithms: Review and the suitable low-cost embedded board for each algorithm". *Journal of Cleaner Production*, *246*(118983), 118983., 2020.

[21] Tang S, Sun Y, Chen Y, Zhao Y, Yang Y, Szeto W. "An enhanced MPPT method combining fractional-order and fuzzy logic control". *IEEE Journal of Photovoltaics*, *7*(2), 640–650, 2017.

[22] Roy RB, Rokonuzzaman M, Amin N, Mishu MK, Alahakoon S, Rahman S, Mithulananthan N, Rahman KS, Shakeri M, Pasupuleti J. "A comparative performance analysis of ANN algorithms for MPPT energy harvesting in solar PV system". *IEEE Access: Practical Innovations, Open Solutions*, *9*, 102137–102152, 2021.

[23] Nguimfack-Ndongmo JD, Harrison A, Alombah NH, Kuate-Fochie R, Ajesam Asoh D, Kenné G. "Adaptive terminal synergetic-backstepping technique based machine learning regression algorithm for MPPT control of PV systems under real climatic conditions". *ISA Transactions*, *145*, 423–442, 2024.

[24] Zhou L, Chen Y, Guo K, Jia F. “New approach for MPPT control of photovoltaic system with mutative-scale dual-carrier chaotic search”. *IEEE Transactions on Power Electronics*, *26*(4), 1038–1048, 2011.

[25] Samantara S, Roy B, Sharma R, Rout A. “Modeling and simulation of CUK converter with beta (B) MPPT for standalone PV system”. *Michael Faraday IET International Summit 2015*, 112 (5.) -112 (5), 2015.

[26] Xu S, Gao Y, Zhou G, Mao G. “A global maximum power point tracking algorithm for photovoltaic systems under partially shaded conditions using modified maximum power trapezium method”. *IEEE Transactions on Industrial Electronics (1982)*, *68*(1), 370–380, 2021.

[27] Osmani K, Haddad A, Lemenand T, Castanier B, Ramadan M. “An investigation on maximum power extraction algorithms from PV systems with corresponding DC-DC converters”. *Energy (Oxford, England)*, *224*(120092), 120092, 2021.

[28] Furtado AMS, Bradaschia F, Cavalcanti MC, Limongi LR. “A reduced voltage range global maximum power point tracking algorithm for photovoltaic systems under partial shading conditions”. *IEEE Transactions on Industrial Electronics (1982)*, *65*(4), 3252–3262, 2018.

[29] Eltamaly AM, Farh HMH. “Dynamic global maximum power point tracking of the PV systems under variant partial shading using hybrid GWO-FLC”. *Solar Energy (Phoenix, Ariz.)*, *177*, 306–316, 2019.

[30] Seyedmahmoudian M, Rahmani R, Mekhilef S, Maung Than Oo A, Stojcevski A, Soon TK, Ghandhari AS. “Simulation and hardware implementation of new maximum power point tracking technique for partially shaded PV system using hybrid DEPSO method”. *IEEE Transactions on Sustainable Energy*, *6*(3), 850–862, 2015.

[31] Sundareswaran K, Vignesh kumar V, Palani S. “Application of a combined particle swarm optimization and perturb and observe method for MPPT in PV systems under partial shading conditions”. *Renewable Energy*, *75*, 308–317, 2015.

[32] Mohanty S, Subudhi B, Ray PK. “A grey wolf-assisted perturb & observe MPPT algorithm for a PV system”. *IEEE Transactions on Energy Conversion*, *32*(1), 340–347, 2017.

[33] Cruz-Duarte JM, Amaya I, Ortiz-Bayliss JC, Conant-Pablos SE, Terashima-Marín H, Shi Y. “Hyper-Heuristics to customise metaheuristics for continuous optimization”. *Swarm and Evolutionary Computation*, *66*(100935), 100935, 2021.

[34] Karmouni H, Chouiekh M, Motahhir S, Qjidaa H, Ouazzani Jamil M, Sayyouri M. “A fast and accurate sine-cosine MPPT algorithm under partial shading with implementation using arduino board”. *Cleaner Engineering and Technology*, *9*(100535), 100535, 2022.

[35] Chandrasekharan S, Subramaniam S, Veerakgoundar V. “Honey badger optimization algorithm based maximum power point tracking for solar photovoltaic systems”. *Electric Power Systems Research*, *221*(109393), 109393, 2023.

[36] Fares D, Fathi M, Shams I, Mekhilef S. “A novel global MPPT technique based on squirrel search algorithm for PV module under partial shading conditions”. *Energy Conversion and Management*, *230*(113773), 113773, 2021.

[37] Mansoor M, Mirza AF, Ling Q. “Harris hawk optimization-based MPPT control for PV systems under partial shading conditions”. *Journal of Cleaner Production*, *274*(122857), 122857, 2020.

[38] Alshareef MJ. “An effective falcon optimization algorithm based MPPT under partial shaded photovoltaic systems”. *IEEE Access: Practical Innovations, Open Solutions*, *10*, 131345–131360, 2022.

[39] Zhao Z, Zhang M, Zhang Z, Wang Y, Cheng R, Guo J, Yang P, Lai CS, Li P, Lai LL. “Hierarchical pigeon-inspired optimization-based MPPT method for photovoltaic systems under complex partial shading conditions”. *IEEE Transactions on Industrial Electronics (1982)*, *69*(10), 10129–10143,2022.

[40] Moosavi SKR, Mansoor M, Zafar MH, Khan NM, Mirza AF, Akhtar N. “Highly efficient maximum power point tracking control technique for PV system under dynamic operating conditions”. *Energy Reports*, *8*, 13529–13543, 2022.

[41] Sridhar R, Subramani C, Pathy S. “A grasshopper optimization algorithm aided maximum power point tracking for partially shaded photovoltaic systems”. *Computers & Electrical Engineering: An International Journal*, *92*(107124), 107124, 2021.

[42] Pervez I, Shams I, Mekhilef S, Sarwar A, Tariq M, Alamri B. “Most valuable player algorithm based maximum power point tracking for a partially shaded PV generation system”. *IEEE Transactions on Sustainable Energy*, *12*(4), 1876–1890, 2021.

[43] Xu H, Zhao M, Xue F, Zhang X, Sun L. “An improved mayfly algorithm with shading detection for MPPT of photovoltaic systems”. *IEEE Access: Practical Innovations, Open Solutions*, *11*, 110827–110836, 2023.

[44] Koh JS, Tan RHG, Lim WH, Tan NML. “A modified particle swarm optimization for efficient maximum power point tracking under partial shading condition”. *IEEE Transactions on Sustainable Energy*, *14*(3), 1822–1834, 2023.

[45] Mohammed KK, Buyamin S, Shams I, Mekhilef S. “Hybrid global maximum power tracking method with partial shading detection technique for PV systems”. *IEEE Journal of Emerging and Selected Topics in Power Electronics*, *10*(4), 4821–4831, 2022.

[46] Azli H, Titri S, Larbes C, Kaced K, Femmam K. “Novel yellow saddle goatfish algorithm for improving performance and efficiency of PV system under partial shading conditions”. *Solar Energy (Phoenix, Ariz.)*, *247*, 295–307, 2022.

[47] Fu C, Zhang L. “A novel method based on tuna swarm algorithm under complex partial shading conditions in PV system”. *Solar Energy (Phoenix, Ariz.)*, *248*, 28–40, 2022.

[48] Refaat A, Ali QA, Elsakka MM, Elhenawy Y, Majozi T, Korovkin NV, Elfar MH. “Extraction of maximum power from PV system based on horse herd optimization MPPT technique under various weather conditions”. *Renewable Energy*, *220*(119718), 119718, 2024.

[49] Mirza AF, Mansoor M, Ling Q. “A novel MPPT technique based on Henry gas solubility optimization”. *Energy Conversion and Management*, *225*(113409), 113409, 2020.

[50] Zheng S, Shahzad M, Asif HM, Gao J, Muqeet HA. “Advanced optimizer for maximum power point tracking of photovoltaic systems in smart grid: A roadmap towards clean energy technologies”. *Renewable Energy*, *206*, 1326–1335, 2023

[51] Mirza AF, Mansoor M, Ling Q, Yin B, Javed MY. “A Salp-Swarm Optimization based MPPT technique for harvesting maximum energy from PV systems under

partial shading conditions". *Energy Conversion and Management*, *209*(112625), 112625, 2020.
[52] Tagayi RK, Baek J, Kim J. "Flower pollination global peak search algorithm for partially shaded solar photovoltaic system". *Journal of Building Engineering*, *66*(105818), 105818, 2023.
[53] Gürkan E, Güner A. "Comparative performance analysis of metaheuristic algorithms for maximum power point tracking under partial shading conditions in PV systems," Pamukkale University Journal of Engineering Sciences, vol. 30, no. 7, pp. 891–905, 2024.
[54] Wolpert DH, Macready WG. "No free lunch theorems for optimization". IEEE Transactions on Evolutionary Computation: A Publication of the IEEE Neural Networks Council, 1(1), 67–82, 1997.
[55] Demirtas M, Koc K. "Parameter extraction of photovoltaic cells and modules by INFO algorithm". *IEEE Access: Practical Innovations, Open Solutions*, *10*, 87022–87052, 2022.
[56] Ahmadianfar I, Heidari AA, Noshadian S, Chen H, Gandomi AH. "INFO: An efficient optimization algorithm based on weighted mean of vectors". *Expert Systems with Applications*, *195*(116516), 116516, 2022.
[57] Zhao W, Wang L, Zhang Z, Fan H, Zhang J, Mirjalili S, Khodadadi N, Cao Q. "Electric eel foraging optimization: A new bio-inspired optimizer for engineering applications". *Expert Systems with Applications*, *238* (122200), 122200, 2024.
[58] Ferahtia S, Houari A, Rezk H, Djerioui A, Machmoum M, Motahhir S, Ait-Ahmed M. "Red-tailed hawk algorithm for numerical optimization and real-world problems". *Scientific Reports*, *13*(1), 1–42, 2023.
[59] Das B, Mukherjee V, Das D. "Student psychology based optimization algorithm: A new population based optimization algorithm for solving optimization problems". *Advances in Engineering Software (Barking, London, England: 1992)*, *146*(102804), 102804, 2020.
[60] Eberhart R, Kennedy J. "A new optimizer using particle swarm theory". MHS'95. Proceedings of the Sixth International Symposium on Micro Machine and Human Science, 39–43, 2022.
[61] He K, Zhang Y, Wang YK, Zhou RH, Zhang HZ. "EABOA: Enhanced adaptive butterfly optimization algorithm for numerical optimization and engineering design problems". *Alexandria Engineering Journal*, *87*, 543–573,2024.
[62] Derrac J, García S, Molina D, Herrera F. "A practical tutorial on the use of nonparametric statistical tests as a methodology for comparing evolutionary and swarm intelligence algorithms". *Swarm and Evolutionary Computation*, *1*(1), 3–18, 2011.